A 2-D Kinetic Theory for Flows of Monodomain Polymer-Rod Nanocomposites

M. Gregory Forest[1], Qingqing Liao[2] and Qi Wang[3,*]

[1] *Department of Mathematics, University of North Carolina at Chapel Hill, Chapel Hill, NC 27599, USA.*

[2] *Department of Mathematics, University of South Carolina, Columbia, SC 29208, USA.*

[3] *Department of Mathematics and NanoCenter at USC, University of South Carolina, Columbia, SC 29208, USA.*

Abstract. We merge classical kinetic theories [M. Doi and S. F. Edwards, The Theory of Polymer Dynamics, 1986] for viscous dispersions of rigid rods, extended to semi-flexibility [A. R. Khokhlov and A. N. Semenov, Macromolecules, 17 (1984), pp. 2678-2685], and for Rouse flexible chains to model the hydrodynamics of polymer nano-rod composites (PNCs). A mean-field potential for the polymer-rod interface provides the key coupling between the two phases. We restrict this first study to two-dimensional conformational space. We solve the coupled set of Smoluchowski equations for three benchmark experiments. First we explore how rod semi-flexibility and the polymer-rod interface alter the Onsager equilibrium phase diagram. Then we determine monodomain phase behavior of PNCs for imposed simple elongation and shear, respectively. These results inform the effects that each phase has on the other as parametric strengths of the interactions are varied in the context of the most basic rheological experiments.

1 Introduction

Polymer-nanoparticle composites are made from blends of flexible polymers and various anisotropic nanoparticles, including nano-clay platelets and graphene sheets, carbon

---

*Corresponding author. *Email addresses:* `forest@amath.unc.edu` (M. G. Forest), `liaoq@mailbox.sc.edu` (Q.-Q. Liao), `qwang@math.sc.edu` (Q. Wang)

nanotubes, nanowires, and metals. They have shown promising, extraordinary properties in chemical, electrical, environmental, and thermal transport as well as ultrahigh mechanical strength. We refer to various review articles [9,18,21–24,27] on the promising diverse applications of polymer nanocomposites.

Given the promising applications of blends of flexible polymers and nanoparticles, a thorough understanding of their phase behavior, dynamics, morphology development and mesoscopic structure evolution, and the full spectrum of rheological behavior in processing conditions, becomes important. Yet theoretical studies of these aspects of polymer blends are sparse. Liu and Fredrickson developed a mean field thermodynamic theory to study phase separation kinetics focusing on low frequency and long wave behavior [16]. Muratov and E proposed a kinetic theory for the incompressible mixture of flexible polymers and rodlike liquid crystalline polymers [8, 19], in which they investigated the phase separation kinetics employing a gradient expansion of the density function of the rodlike liquid crystalline polymer and identified various transitions leading to phase separation including a micro-phase separation transition. In both of these theories, the detailed conformational dynamics of the flexible polymers and the semiflexibility of the rods are ignored. There is now overwhelming evidence that the polymer phase is modified due to surface chemistry with the rod phase, and the local rod-polymer interactions are critical elements of a predictive theory. This paper takes into account the local conformational dynamics of the blend of the flexible polymer and the semiflexible nanorod in a hydrodynamic theory in a 2-D configurational space setting.

Two recent research papers have proposed continuum models of nanorods and nanoclays based on the GENERIC formalism [10,20]. The models yield a reasonable qualitative agreement with experimental data. To explore more detailed microscopic information and their role in mesoscopic material properties, our aim is to develop a kinetic theory for flowing polymer nanoparticle dispersion systematically accounting for the conformational dynamics of the flexible polymer, the polymer nano-particle interactions and semiflexibility of the nano-particles [12]. This theory extends work of the authors on blends of polymers and rodlike liquid crystals [14], and of Semenov and Khoklov on semiflexible liquid crystal polymers [15].

In the blend system, we introduce a statistical weight for the flexible polymer matrix $\Theta(\mathbf{x},\{\mathbf{R}_i\},t)$, where $\mathbf{x}$ is the location of the material point, t is time, and $\{\mathbf{R}_i\}=(\mathbf{R}_1,\cdots,\mathbf{R}_n)$ describes the conformation of the flexible polymer chain modeled as a bead-spring chain [1,3]. We assume

$$\Theta=\phi\theta(\mathbf{x},\{\mathbf{R}_i\},t),\tag{1.1}$$

where θ is a probability density function for the conformation of the bead-spring chain and ϕ is the volume fraction of the polymer per unit volume at the macroscopic level. The time evolution of θ is governed by the Rouse dynamics while ϕ is a constant in the monodomain case considered here. Since the added conformational dynamics is local, it does not affect the macroscopic incompressibility constraint. It does however add a detailed conformational contribution of the flexible polymer to the elastic stress as well as to

the orientational dynamics of the nano-particle phase. Within the framework presented here, FENE, FENE-p, and Giesekus etc. models can all be cast in this kinetic theory for the dynamics of the flexible polymer. In principle, it can be extended to deal with arbitrary shaped nano-particles as well [4–7].

Specifically, this paper aims at:

- casting the kinetic theory in a 2-D configurational space with a 2-D bead-spring model for the polymer matrix and a semi-flexible rod for the nano-particle ensemble with excluded volume interactions;

- studying the solution of the highly nonlinear Smoluchowski equation in simple benchmark flows to explore the effect of various materials parameters such as the semiflexibility and the interfacial interaction between the polymer and the nanorod.

The rest of the paper is organized into five sections. First, we develop the theory with a nonlocal intermolecular potential accounting for the Brownian motion, excluded volume effects, conformational entropic effect for semiflexible nanorods, and polymer nanorod interaction. We then study the PNC model in equilibrium, elongation and simple shear flows to investigate the phase diagram and rheological responses.

2 Hydrodynamic theory

We derive the kinetic theory for flowing polymer-nanorod nanocomposites in 2-D configurational space in this section. For incompressible mixtures of flexible polymers and semiflexible nanorods, we introduce (i) the probability density function (PDF) of nanorods per unit volume $f(\mathbf{x},\mathbf{m},t)$ at $(\mathbf{x},t)$ with the mean orientation axis $\mathbf{m}$; and, (ii) another statistical weight proportional to the number density of flexible polymers (modeled as bead-spring chains) per unit volume $\Theta(\mathbf{x},\mathbf{q},t)$ at $(\mathbf{x},t)$ with the chain conformation $\mathbf{q}$ (the end-to-end vector of a bead-spring model). We assume Θ is scaled into,

$$\Theta(\mathbf{x},\mathbf{q},t) = \phi\theta(\mathbf{x},\mathbf{q},t), \tag{2.1}$$

where ϕ is the volume fraction of the flexible polymer modeled as a bead-spring chain and $\theta(\mathbf{x},\mathbf{q},t)$ is the probability density function (pdf) of the chain, i.e.,

$$\int \theta(\mathbf{x},\mathbf{q},t)d\mathbf{q} = 1. \tag{2.2}$$

We denote the ensemble average with respect to the probability density function (PDF) θ by

$$\ll(\bullet)\gg = \int(\bullet)\theta(\mathbf{x},\mathbf{q},t)d\mathbf{q} \tag{2.3}$$

and the ensemble average with respect to the PDF of the nanorod $f(\mathbf{m},\mathbf{x},t)$ by

$$\langle(\bullet)\rangle = \int_{\|\mathbf{m}\|=1}(\bullet)f(\mathbf{x},\mathbf{m},t)d\mathbf{m}. \tag{2.4}$$

We propose a free energy functional for the mixture of polymers and semiflexible nanorods consisting of three parts: (i) free energy associated with the Brownian motion of the nanorods, entropic contribution due to semiflexibility and excluded volume interaction among the nanorods, (ii) Brownian motion and the elastic energy for bead-spring chains, and (iii) the free energy due to the surface contact interaction between the nanorods and flexible polymer molecules. The excluded volume interaction for the flexible polymers can be easily accounted for by adding an additional excluded volume potential for bead-spring chains in the free energy, which has a negligible contribution to the elastic stress [3]. For the sake of simplicity, we neglect this effect in the current derivation. In the following, we assume the nanorods are monodispersed ellipses, where the semiflexibility of the ellipses are taken into account separately, the flexible polymer matrix consists of bead-spring chains of uniform molecular weight, and the effects of gelation, excluded volume interaction between nanorods and polymers, poly-dispersity and polymerization of the flexible polymers are ignored.

Free energy

Let $A[f]$ denote the free energy of the mixture in a material volume Ω,

$$A[f,\theta] = F_{nr} + F_{beads} + F_{int}, \tag{2.5}$$

where F_{nr} is the free energy associated with the semiflexible nanorods, F_{beads} is the free energy associated with the conformational change of the flexible polymer modeled as a bead-spring chain, and F_{int} is the free energy due to the polymer-nanorod contact interaction.

Specifically, the free energy for the nanorods consists of a linear combination of the rigid rod rotational entropic potential and semiflexible rigid body conformational entropic potential along with the rod excluded volume potential

$$F_{nr} = ckT(1-\phi)\int_\Omega \int_{\|\mathbf{m}\|=1} [(1-r_f)(f(\mathbf{m},\mathbf{x},t)\ln f(\mathbf{m},\mathbf{x},t) - f(\mathbf{m},\mathbf{x},t))$$

$$+r_f L_r f\|\mathcal{R}\ln f\|^2 + \frac{1}{2}U(\mathbf{m},\mathbf{x},t)f(\mathbf{m},\mathbf{x},t)]d\mathbf{m}d\mathbf{x}, \tag{2.6}$$

where c is the number density of the nanorods, r_f is an interpolating parameter between 0 and 1 parameterizing the degree of semi-flexibility of the nanorod (an important model parameter to be explored exclusively later), $L_r > 0$ is proportional to the ratio of the contour length of the nanorod to the persistent length of the nanorod [15], k is the Boltzmann constant, T is the absolute temperature, $U(\mathbf{m},\mathbf{x},t)$ is the excluded volume potential defined below, and $\mathcal{R} = (\mathbf{I} - \mathbf{mm}) \cdot \frac{\partial}{\partial \mathbf{m}}$ is the orientational gradient operator.

The flexible bulk free energy for the polymer chain is given by the chain Brownian motion and the elastic potential.

$$F_{beads} = kT\gamma\phi\int_\Omega \int [\theta(\mathbf{x},\mathbf{q},t)\ln\theta(\mathbf{x},\mathbf{q},t) + \xi\|\mathbf{q}\|^2\theta(\mathbf{x},\mathbf{q},t)]d\mathbf{q}d\mathbf{x}, \tag{2.7}$$

where $\gamma kT\xi$ is the spring constant for the Rouse chain and γ is a reciprocal volume parameter ($1/\gamma$ is proportional to the effective area of a polymer molecule). We remark that a FENE type potential can be used as well, where the potential is given by

$$F_{beads} = kT\gamma\phi \int_\Omega \int [\theta(\mathbf{x},\mathbf{q},t)ln\theta(\mathbf{x},\mathbf{q},t) - \frac{\xi d_0^2}{2} ln(1 - \|\mathbf{q}\|^2/d_0^2)\theta(\mathbf{x},\mathbf{q},t)]d\mathbf{q}d\mathbf{x}, \qquad (2.8)$$

where d_0 is the maximum extensible length for the segment of the polymer chain.

The polymer-nanorod interaction potential is made up of the polymer-nanorod contact interaction,

$$F_{int} = c\phi(1-\phi)kT\gamma \int_\Omega \int_{\|\mathbf{m}\|=1} [\alpha_1((\mathbf{q})\cdot\mathbf{m})^2 + \alpha_2((\mathbf{q})\times\mathbf{m})^2]\theta(\mathbf{x},\mathbf{q},t)f(\mathbf{m},\mathbf{x},t)d\mathbf{q}d\mathbf{m}d\mathbf{x}, \quad (2.9)$$

where α_1 and α_2 parameterize the normal and tangential interaction, respectively.

Configurational kinetics

We neglect the translational diffusion of the material and instead focus only on the configurational space diffusion in the monodomain. The chemical potential for the nanorod is defined by μ_{nr},

$$\mu_{nr} = \frac{\delta A}{c(1-\phi)\delta f} = kT\left((1-r_f)lnf + r_f L_r\left[\|\mathcal{R}lnf\|^2 - 2\frac{\mathcal{R}\cdot(f\mathcal{R}lnf)}{f}\right] + U\right)$$
$$+ \gamma kT\phi \int[\alpha_1((\mathbf{q})\cdot\mathbf{m})^2 + \alpha_2((\mathbf{q})\times\mathbf{m})^2]\theta d\mathbf{q}. \qquad (2.10)$$

The rotary flux in the configurational space $\mathbf{m} \in S^1$ for the nanorod is given by

$$\mathbf{j}_\mathbf{m}^r = -\frac{1}{kT}fD_r(\mathbf{m})\cdot\mathcal{R}\mu_{nr}, \qquad (2.11)$$

where $D_r(\mathbf{m})$ is the rotary diffusivity, a scalar in this paper. Analogously, the flux of the flexible polymer in the conformational space $\mathbf{q}$ is given by

$$(\mathbf{j}_\theta) = -\mathbf{H}\cdot\frac{\partial}{\partial\mathbf{q}}\mu_\theta, \qquad (2.12)$$

where $\mathbf{H}$ is the mobility matrix for the bead-spring chain [3], and the chemical potential for the local polymer chain is given by

$$\mu_\theta = \frac{1}{\gamma\phi}\frac{\delta A}{\delta\theta} = kT[ln\theta + 1 + \xi\|\mathbf{q}\|^2] + kT\int_{\|\mathbf{m}\|=1}[\alpha_1((\mathbf{q})\cdot\mathbf{m})^2 + \alpha_2((\mathbf{q})\times\mathbf{m})^2]c(1-\phi)fd\mathbf{m}]$$
$$= kT[ln\theta + (\xi + c(1-\phi)\alpha_2)\|\mathbf{q}\|^2 + c(1-\phi)(\alpha_1-\alpha_2)\mathbf{q}\mathbf{q}:\langle\mathbf{m}\mathbf{m}\rangle] + const. \qquad (2.13)$$

Smoluchowski equation

Given the above fluxes due to the rotary diffusion of each constituent in the nanocomposite and taking into account the spatial convection as well as the rotary convection [3], we arrive at the Smoluchowski equation for $f(\mathbf{m},\mathbf{x},t)$ as follows:

$$\frac{df}{dt} = \mathcal{R}\cdot\left(\frac{D_r(\mathbf{m})}{kT}f\mathcal{R}\mu_{nr}\right) - \mathcal{R}\cdot(\dot{\mathbf{m}}f),$$

$$\dot{\mathbf{m}} = \mathbf{W}\cdot\mathbf{m} + a[\mathbf{D}\cdot\mathbf{m} - \mathbf{D}:\mathbf{mmm}],$$

(2.14)

where $\mathbf{W} = \frac{1}{2}(\mathbf{K}-\mathbf{K}^T), \mathbf{D} = \frac{1}{2}(\mathbf{K}+\mathbf{K}^T)$ are the vorticity and rate of strain tensor, respectively, $K = \nabla\mathbf{v}$ is the velocity gradient tensor, $0 \leq a \leq 1$ is the standard rod shape parameter, and $\frac{d}{dt} = \frac{\partial}{\partial t} + \mathbf{v}\cdot\nabla$ is the material derivative. Analogously, we obtain the accompanying Smoluchowski equation for θ

$$\frac{d}{dt}\theta = -\frac{\partial}{\partial\mathbf{q}}\cdot((\mathbf{K}-(1-a_0)\mathbf{D})\cdot\mathbf{q}\theta) + \frac{\partial}{\partial\mathbf{q}}\cdot\mathbf{H}\cdot\left(\frac{\partial}{\partial\mathbf{q}}\theta\mu_\theta\right),$$

(2.15)

where $-1 \leq a_0 \leq 1$ is a rate parameter describing the extent of the nonaffine motion. For isotropic friction, $\mathbf{H} = \frac{1}{\zeta_p}\mathbf{I}$, where ζ_p is the friction coefficient. In order to couple the kinetic equation for the momentum transport process in the macroscopic flow, we need the stress tensor for the mixture [25, 26].

Stress tensor

The extra stress is given by two parts, the viscous stress τ_v and the elastic stress τ_e:

$$\tau = \tau_v + \tau_e.$$

(2.16)

We consider two sources for the viscous stress in this theory. There must be a zero-strain-rate viscosity while the mixture is isotropic, which we denote as η_v. The viscous stress associated to this effect is denoted as $2\eta_v\mathbf{D}$. In addition, there is a viscous stress due to the friction between polymers and nanorods. Following the procedure outlined in [25], we arrive at the viscous stress

$$2c(1-\phi)kT\zeta\mathbf{D}:\langle\mathbf{mmmm}\rangle + c\zeta_2(1-\phi)kT(\mathbf{D}\cdot\langle\mathbf{mm}\rangle + \langle\mathbf{mm}\rangle\cdot\mathbf{D}),$$

where ζ and ζ_2 are two friction parameters. The overall viscous stress is therefore given by

$$\tau_v = 2\eta_v D + 2c(1-\phi)kT\zeta\mathbf{D}:\langle\mathbf{mmmm}\rangle + c(1-\phi)\zeta_2 kT(\mathbf{D}\cdot\langle\mathbf{mm}\rangle + \langle\mathbf{mm}\rangle\cdot\mathbf{D}).$$

(2.17)

The elastic stress and extra elastic body force are derived through a virtual work principle [3]. Consider an infinitesimal displacement given by $\delta\mathbf{u} = \mathbf{v}\delta t$ corresponding to a

deformation rate $\delta\epsilon = K\delta t$. The variation of the free energy (2.5) in response to the infinitesimal deformation and displacement is equal to the work done by a body force along the displacement and the stress with respect to the deformation rate:

$$\delta A = \int_\Omega [\delta\epsilon : \tau_e - \delta\mathbf{u}\cdot\mathbf{F}_e]d\mathbf{x}, \tag{2.18}$$

where $\mathbf{F}_e$ is the elastic body force induced by the long range interaction among the nanorods and polymer-nanorod interaction. It follows from a simple calculation that

$$\mathbf{F}_e = -\nabla p_0, \tag{2.19}$$

where p_0 is a scalar function, and

$$\tau_e = \gamma\phi\left[\frac{a_0}{2}[\ll\frac{\partial\mu_\theta}{\partial\mathbf{q}}\mathbf{q}\gg + \ll\mathbf{q}\frac{\partial\mu_\theta}{\partial\mathbf{q}}\gg] + \frac{1}{2}[\ll\frac{\partial\mu_\theta}{\partial\mathbf{q}}\mathbf{q}\gg - \ll\mathbf{R}\frac{\partial\mu_\theta}{\partial\mathbf{q}}\gg]\right]$$
$$+\frac{ac(1-\phi)}{2}[\langle\mathcal{R}(\mu_{nr})\mathbf{m}\rangle + \langle\mathbf{m}\mathcal{R}(\mu_{nr})\rangle] + \frac{c(1-\phi)}{2}[\langle\mathcal{R}(\mu_{nr})\mathbf{m}\rangle - \langle\mathbf{m}\mathcal{R}(\mu_{nr})\rangle]. \tag{2.20}$$

Since p_0 can be identified as a part of the hydrodynamic pressure in the incompressible system, we will not explicitly write the elastic external force in the momentum balance equation in the following. We note that

$$\ll\frac{\partial\mu_\theta}{\partial\mathbf{q}}\mathbf{q}\gg$$
$$= 2kT[(\xi+c(1-\phi)\alpha_2)\ll\mathbf{qq}\gg + (\alpha_1-\alpha_2)c(1-\phi)\langle\mathbf{mm}\rangle\cdot\ll\mathbf{qq}\gg] + scalar\mathbf{I}. \tag{2.21}$$

The total extra stress, modulo a pressure like term, is then given by

$$\tau = \tau_v + \tau_e$$
$$= 2\eta_v D + 2c(1-\phi)kT\zeta\mathbf{D}:\langle\mathbf{mmmm}\rangle + c(1-\phi)\zeta_2 kT(\mathbf{D}\cdot\langle\mathbf{mm}\rangle + \langle\mathbf{mm}\rangle\cdot\mathbf{D})$$
$$+\frac{ac(1-\phi)}{2}[\langle\mathcal{R}(\mu_{nr})\mathbf{m}\rangle + \langle\mathbf{m}\mathcal{R}(\mu_{nr})\rangle] + \frac{c(1-\phi)}{2}[\langle\mathcal{R}(\mu_{nr})\mathbf{m}\rangle - \langle\mathbf{m}\mathcal{R}(\mu_{nr})\rangle]$$
$$+2a_0\gamma kT\phi(\xi+c(1-\phi)\alpha_2)\ll\mathbf{qq}\gg + \gamma c(1-\phi)\phi kT[(\alpha_1-\alpha_2)[a_0[\langle\mathbf{mm}\rangle\cdot\ll\mathbf{qq}\gg$$
$$+\ll\mathbf{qq}\gg\cdot\langle\mathbf{mm}\rangle] + \langle\mathbf{mm}\rangle\cdot\ll\mathbf{qq}\gg - \ll\mathbf{qq}\gg\cdot\langle\mathbf{mm}\rangle]. \tag{2.22}$$

Governing equations

The Smoluchowski equation, the stress constitutive equation, the continuity equation and the balance of linear momentum equation constitute the governing system of equations for flows of the polymer-nanorod composite in the kinetic theory, which are summarized below.

Continuity equation

$$\frac{d}{dt}\rho + \rho\nabla\cdot\mathbf{v} = 0. \tag{2.23}$$

Balance of linear momentum

$$\rho\dot{\mathbf{v}} = \nabla\cdot(-p\mathbf{I}+\tau)+\rho\mathbf{g}, \tag{2.24}$$

where p is the hydrodynamic pressure, and $\mathbf{g}$ is the external force per unit mass. Smoluchowski kinetic equations

$$\begin{cases} \dfrac{df}{dt} = \mathcal{R}\cdot(\dfrac{D_r(\mathbf{m})}{kT}f\mathcal{R}\mu) - \mathcal{R}\cdot(\mathbf{m}\times\dot{\mathbf{m}}f), \\[2mm] \dot{\mathbf{m}} = \mathbf{W}\cdot\mathbf{m} + a[\mathbf{D}\cdot\mathbf{m} - \mathbf{D}:\mathbf{mmm}], \\[2mm] \dfrac{d}{dt}\theta = -\dfrac{\partial}{\partial\mathbf{q}}\cdot((\mathbf{K}-(1-a_0)\mathbf{D})\cdot\mathbf{q}\theta) + \dfrac{\partial}{\partial\mathbf{q}}\cdot\mathbf{H}\cdot(\dfrac{\partial}{\partial\mathbf{q}}\mu_\theta\theta), \end{cases} \tag{2.25}$$

Stress constitutive equation

$$\begin{aligned} \tau ={}& 2\eta_v D + 2kT\zeta(1-\phi)\mathbf{D}:\langle\mathbf{mmmm}\rangle + \zeta_2 kT(1-\phi)(\mathbf{D}:\langle\mathbf{mm}\rangle + \langle\mathbf{mm}\rangle\cdot\mathbf{D}) \\ &+ \frac{ac(1-\phi)}{2}[\langle\mathcal{R}(\mu_{nr})\mathbf{m}\rangle + \langle\mathbf{m}\mathcal{R}(\mu_{nr})\rangle] + \frac{c(1-\phi)}{2}[\langle\mathcal{R}(\mu_{nr})\mathbf{m}\rangle - \langle\mathbf{m}\mathcal{R}(\mu_{nr})\rangle] \\ &+ 2a_0\gamma kT\phi(\xi+\alpha_2 c(1-\phi))\ll\mathbf{qq}\gg + \gamma c\phi(1-\phi)kT[(\alpha_1-\alpha_2)[a_0[\langle\mathbf{mm}\rangle\cdot\ll\mathbf{qq}\gg \\ &+ \ll\mathbf{qq}\gg\cdot\langle\mathbf{mm}\rangle] + \langle\mathbf{mm}\rangle\cdot\ll\mathbf{qq}\gg - \ll\mathbf{qq}\gg\cdot\langle\mathbf{mm}\rangle]. \end{aligned} \tag{2.26}$$

3   Model reduction for Rouse chains and Smoluchowski equations in elongation and shear flows

This kinetic theory consists of two Smoluchowski equations. If we adopt an isotropic tensor for the polymer mobility matrix $\mathbf{H}=\frac{1}{\zeta_p}\mathbf{I}$, we can bypass the Smoluchowski equation for θ [1]. Taking the second moment of $\mathbf{q}$ with respect to pdf θ, we arrive at the evolution equation for the structure tensor of the flexible polymer $\ll\mathbf{qq}\gg$:

$$\begin{aligned} &\frac{d}{dt}\ll\mathbf{qq}\gg - \mathbf{W}\cdot\ll\mathbf{qq}\gg + \ll\mathbf{qq}\gg\cdot\mathbf{W} - a_0[\mathbf{D}\cdot\ll\mathbf{qq}\gg + \ll\mathbf{qq}\gg\cdot\mathbf{D}] \\ &= \frac{2kT}{\zeta_p}\mathbf{I} - \frac{4(\xi+c(1-\phi)\alpha_2)kT}{\zeta_p}\ll\mathbf{qq}\gg \\ &\quad - \frac{2c(1-\phi)(\alpha_1-\alpha_2)kT}{\zeta_p}[\mathbf{Q}\cdot\ll\mathbf{qq}\gg + \ll\mathbf{qq}\gg\cdot\mathbf{Q}], \end{aligned} \tag{3.1}$$

where the second moment is denoted as

$$\mathbf{Q}=\langle\mathbf{mm}\rangle.$$

This equation for $\mathbf{Q}$ generalizes the Johnson-Segalman model [1] to include the coupling terms between nanorods and polymers. With this self-contained equation, we can completely bypass the Smoluchowski equation for pdf θ now. We remark that if the FENE type elastic potential is used, the decoupling is not feasible.

To simplify the stress expression, we introduce a scaled structure tensor for the flexible polymer

$$\mathbf{U} = 2\gamma kT(\xi + c(1-\phi)\alpha_2) \ll \mathbf{qq} \gg.$$ (3.2)

It follows from the governing equation for the structure tensor $\ll \mathbf{q}_i\mathbf{q}_i \gg$ (3.1) that

$$\lambda\left[\frac{d}{dt}\mathbf{U} - \mathbf{W}\cdot\mathbf{U} + \mathbf{U}\cdot\mathbf{W} - a_0[\mathbf{D}\cdot\mathbf{U} + \mathbf{U}\cdot\mathbf{D}]\right] + \mathbf{U} = \epsilon_p\mathbf{I} - \beta(1-\phi)[\mathbf{Q}\cdot\mathbf{U} + \mathbf{U}\cdot\mathbf{Q}],$$ (3.3)

where

$$\lambda = \frac{\zeta_p}{4(\xi + c(1-\phi)\alpha_2)kT}, \quad \epsilon_p = \gamma kT, \quad \beta = \frac{c(\alpha_1 - \alpha_2)}{2(\xi + c(1-\phi)\alpha_2)}$$ (3.4)

are the relaxation time, polymer viscosity, and a dimensionless parameter measuring the degree of the surface contact interaction relative to the modulus of the mixture (a key parameter to be explored extensively in the following), respectively.

We use the Maier-Saupe potential to approximate the excluded volume potential in the following [25]

$$U_{ms} = -N(1-\phi)\mathbf{Q}:\mathbf{mm},$$ (3.5)

where N is a dimensionless concentration related to the geometry of the nanorod. With this excluded volume potential, the chemical potential for the nanorod is explicitly given by

$$\mu_{nr} = kT\left[(1-r_f)lnf + r_f L_r\left((\frac{\partial}{\partial\theta}lnf)^2 - 2\frac{1}{f}\frac{\partial^2}{\partial\theta^2}f\right) + U_{ms} + \frac{\phi\beta}{ckT}\mathbf{U}:\mathbf{mm}\right].$$ (3.6)

Consider an imposed shear flow

$$\mathbf{v} = \begin{pmatrix} \dot{\gamma}y \\ 0 \end{pmatrix}, \quad \mathbf{W} = \frac{\dot{\gamma}}{2}\begin{pmatrix} 0 & 1 \\ -1 & 0 \end{pmatrix}, \quad \mathbf{D} = \frac{\dot{\gamma}}{2}\begin{pmatrix} 0 & 1 \\ 1 & 0 \end{pmatrix},$$ (3.7)

where $\dot{\gamma}$ is the shear rate. We parameterize the unit vector $\mathbf{m}$ by the polar angle θ:

$$\mathbf{m} = (\cos\theta, \sin\theta)$$ (3.8)

and denote its orthogonal counterpart as

$$\mathbf{m}_\perp = (-\sin\theta, \cos\theta).$$ (3.9)

The Smoluchowski equation can be written as

$$\frac{d}{dt}f = \frac{\partial}{\partial\theta}\left[D_r\left((1-r_f)\frac{\partial}{\partial\theta}f + r_f L_r\left(\frac{4f_\theta f_{\theta\theta}}{f} - 2\frac{f_\theta^3}{f^2} - 2f_{\theta\theta\theta}\right)\right.\right.$$
$$\left.\left. + f[(A_{22}-A_{11})\sin2\theta + 2A_{12}\cos2\theta]\right) - \left[\frac{\dot{\gamma}}{2}(a\cos2\theta - 1)f\right]\right],$$ (3.10)

where

$$A = -N(1-\phi)\mathbf{Q} + \frac{\beta\phi}{ckT}\mathbf{U}, \tag{3.11}$$

and the subscript of f denotes partial derivative with respect to θ. For an imposed elongational flow,

$$\mathbf{v} = (\dot{\gamma}x, -\dot{\gamma}y), \tag{3.12}$$

where $\dot{\gamma}$ denotes the elongational rate in this context, the Smoluchowski equation can be written as

$$\frac{d}{dt}f = \frac{\partial}{\partial\theta}\left[D_r\left((1-r_f)\frac{\partial}{\partial\theta}f + r_fL_r\left(\frac{4f_\theta f_{\theta\theta}}{f} - 2\frac{f_\theta^3}{f^2} - 2f_{\theta\theta\theta}\right)\right.\right.$$
$$\left.\left. + f[(A_{22}-A_{11})\sin2\theta + 2A_{12}\cos2\theta]\right) + \left[\dot{\gamma}(a\sin2\theta)f\right]\right]. \tag{3.13}$$

The second moment of $\mathbf{m}$ with respect to the pdf f is evaluated as

$$\mathbf{Q} = \langle\mathbf{mm}\rangle = \int_{\|\mathbf{m}\|=1}\mathbf{mm}f d\mathbf{m} = 2\int_0^\pi\mathbf{mm}fd\theta$$
$$= \int_0^\pi\begin{pmatrix} (1+\cos2\theta) & \sin2\theta \\ \sin2\theta & (1-\cos2\theta) \end{pmatrix}fd\theta. \tag{3.14}$$

The extra stress tensor can be expressed as

$$\tau = 2\eta_v\mathbf{D} + 2ckT\zeta(1-\phi)\mathbf{D}:\langle\mathbf{mmmm}\rangle + \zeta_2 ckT(1-\phi)(\mathbf{D}\cdot\mathbf{Q} + \mathbf{Q}\cdot\mathbf{D})$$
$$+ 2ackT(1-\phi)\left[(1-r_f)(\mathbf{Q} - \frac{1}{2}\mathbf{I}) - N\mathbf{Q}^2 + N\mathbf{Q}:\langle\mathbf{mmmm}\rangle\right.$$
$$\left. + \frac{1}{4}r_fL_r\left(\langle\mathbf{m}_\perp\mathbf{m}\frac{\partial}{\partial\theta}((\frac{f_\theta}{f})^2 - \frac{2}{f}f_{\theta\theta})\rangle + \langle\mathbf{mm}_\perp\frac{\partial}{\partial\theta}((\frac{f_\theta}{f})^2 - \frac{2}{f}f_{\theta\theta})\rangle\right)\right]$$
$$+ \frac{ckT}{2}(1-\phi)r_fL_r\left(\langle\mathbf{m}_\perp\mathbf{m}\frac{\partial}{\partial\theta}((\frac{f_\theta}{f})^2 - \frac{2}{f}f_{\theta\theta})\rangle - \langle\mathbf{mm}_\perp\frac{\partial}{\partial\theta}((\frac{f_\theta}{f})^2 - \frac{2}{f}f_{\theta\theta})\rangle\right)$$
$$+ a_0\phi\mathbf{U} + \phi(1-\phi)\beta\left[a(\mathbf{U}\cdot\mathbf{Q} + \mathbf{Q}\cdot\mathbf{U} - 2\mathbf{U}:\langle\mathbf{mmmm}\rangle) + a_0(\mathbf{Q}\cdot\mathbf{U} + \mathbf{U}\cdot\mathbf{Q})\right]. \tag{3.15}$$

4 Nondimensionalization

We use a characteristic length scale h, time scale t_0, and force scale f_0 to nondimensionalize the governing system of equations for the nanocomposite flow

$$\tilde{\mathbf{v}} = \frac{t_0}{h}\mathbf{v}, \quad \tilde{\tau} = \frac{h^2}{f_0}\tau, \quad \tilde{p} = \frac{h^2}{f_0}p, \quad \tilde{\mathbf{U}} = \frac{h^2}{f_0}\mathbf{U}, \tag{4.1}$$

where the inertial force is used as the characteristic force $f_0 = \rho h^4 / t_0^2$ and the characteristic time t_0 will be chosen later. A group of dimensionless parameters then arise

$$Re = \frac{h^2}{\eta \rho t_0}, \quad \alpha = \frac{ckTh^2}{f_0}, \quad \Lambda_1 = \frac{\lambda_1}{t_0}, \quad E_p = \frac{\epsilon_p h^2}{f_0}, \quad De = \frac{1}{t_0 D_r}, \quad Pe = t_0 \dot\gamma. \tag{4.2}$$

Here Re is the Reynolds number for the solvent, α is a parameter measuring the strength of the thermal force relative to the inertia force, Λ_1 is the Deborah number for the polymer and De is the Deborah number for the nanorod, Pe is the Peclet number due to the imposed linear flow field.

In this paper, we choose the characteristic timescale t_0 as the reciprocal rotational diffusion rate of the rods $t_0 = D_r^{-1}$, so that the dynamics is measured in this unit. This is equivalent in the above scaling to a unit Deborah number for the nanorod phase: $De = 1$. We drop the tilde on the dimensionless variables; then, the dimensionless equations for the nanocomposite flow are given as follows:

$$\nabla \cdot \mathbf{v} = 0, \quad \frac{d\mathbf{v}}{dt} = \nabla \cdot (-p\mathbf{I} + \tau),$$

$$\frac{d}{dt} f = \frac{\partial}{\partial\theta} \left[\frac{1}{De} \left((1-r_f) \frac{\partial}{\partial\theta} f + r_f L_r \left(\frac{4 f_\theta f_{\theta\theta}}{f} - 2 \frac{f_\theta^3}{f^2} - 2 f_{\theta\theta\theta} \right) \right. \right.$$

$$\left. \left. + f[(A_{22} - A_{11}) \sin 2\theta + 2 A_{12} \cos 2\theta] \right) - \left[\frac{Pe}{2} (a \cos 2\theta - 1) f \right] \right], \qquad \text{Shear}$$

$$\frac{d}{dt} f = \frac{\partial}{\partial\theta} \left[\frac{1}{De} \left((1-r_f) \frac{\partial}{\partial\theta} f + r_f L_r \left(\frac{4 f_\theta f_{\theta\theta}}{f} - 2 \frac{f_\theta^3}{f^2} - 2 f_{\theta\theta\theta} \right) \right. \right.$$

$$\left. \left. + f[(A_{22} - A_{11}) \sin 2\theta + 2 A_{12} \cos 2\theta] \right) + [a Pe \sin 2\theta f] \right], \qquad \text{Elongation}$$

$$A = -N(1-\phi)\mathbf{Q} + \frac{\beta\phi}{\alpha}\mathbf{U}, \tag{4.3}$$

$$\tau = 2\eta_v \mathbf{D} + 2\alpha\zeta(1-\phi)\mathbf{D} : \langle \mathbf{mmmm} \rangle + \zeta_2 \alpha (1-\phi)(\mathbf{D} \cdot \mathbf{Q} + \mathbf{Q} \cdot \mathbf{D})$$

$$2a\alpha(1-\phi) \left[(1-r_f)(\mathbf{Q} - \frac{1}{2}\mathbf{I}) - N\mathbf{Q}^2 + N\mathbf{Q} : \langle \mathbf{mmmm} \rangle \right.$$

$$\left. + \frac{1}{4} r_f L_r \left(\langle \mathbf{m}_\perp \mathbf{m} \frac{\partial}{\partial\theta} ((\frac{f_\theta}{f})^2 - \frac{2}{f} f_{\theta\theta}) \rangle + \langle \mathbf{mm}_\perp \frac{\partial}{\partial\theta} ((\frac{f_\theta}{f})^2 - \frac{2}{f} f_{\theta\theta}) \rangle \right) \right]$$

$$+ \frac{\alpha}{2} (1-\phi) r_f L_r \left(\langle \mathbf{m}_\perp \mathbf{m} \frac{\partial}{\partial\theta} ((\frac{f_\theta}{f})^2 - \frac{2}{f} f_{\theta\theta}) \rangle - \langle \mathbf{mm}_\perp \frac{\partial}{\partial\theta} ((\frac{f_\theta}{f})^2 - \frac{2}{f} f_{\theta\theta}) \rangle \right)$$

$$+ a_0 \phi \mathbf{U} + \phi(1-\phi)\beta \left[a(\mathbf{U} \cdot \mathbf{Q} + \mathbf{Q} \cdot \mathbf{U} - 2\mathbf{U} : \langle \mathbf{mmmm} \rangle) + a_0(\mathbf{Q} \cdot \mathbf{U} + \mathbf{U} \cdot \mathbf{Q}) \right],$$

$$\Lambda_1 \left[\frac{d}{dt} \mathbf{U} - \mathbf{W} \cdot \mathbf{U} + \mathbf{U} \cdot \mathbf{W} - a_0 [\mathbf{D} \cdot \mathbf{U} + \mathbf{U} \cdot \mathbf{D}] \right] + \mathbf{U} = E_p \mathbf{I} - \beta(1-\phi)[\mathbf{Q} \cdot \mathbf{U} + \mathbf{U} \cdot \mathbf{Q}].$$

5 Numerical method: collocation method

We numerically solve the nonlinear system of equations given above (Eq. (4.3)) in monodomains. In a monodomain and in cases of equilibrium, simple elongation and shear, the velocity field is either a constant or a linear function of the coordinates such that the continuity and the momentum transport equation are trivially satisfied. We therefore only need to solve the Smoluchowski equation for the nanorods and the constitutive equation for the polymer structure tensor **U** numerically. The stress tensor is postprocessed from the numerical solution of **U** and f, the pdf for the nanorod. Given the nonlinear terms in the Smoluchowski equation, it is advantageous to use the collocation method to discretize the PDE system [2]. We discretize the interval $[0,\pi]$ into n equal intervals with grid points:

$$\theta_j = \frac{1}{2}(jh+\pi), \quad h=\frac{2\pi}{n}, \quad j=-n/2,\cdots,n/2,$$

and approximate the function using the interpolant

$$f_a = \sum_{j=-n/2}^{n/2-1} f_j S_n(2(\theta-\theta_j)), \tag{5.1}$$

where $f_j = f(\theta_j)$ and $S_n(x) = (\sin\frac{nx}{2})/(n\tan\frac{x}{2})$ defined in $(-\pi,\pi)$ is the Sinc function which is an approximate δ function with the property

$$S_n(0)=1. \tag{5.2}$$

Thus,

$$f_a(\theta_j)=f_j, \quad j=-n/2,\cdots,n/2. \tag{5.3}$$

The derivatives evaluated at the grid points are given by

$$f_{a\theta,k}=2\sum_{j=-n/2}^{n/2-1} f_j S_n'(2(\theta_k-\theta_j)), \quad k=-n/2,\cdots,n/2-1, \tag{5.4}$$

where the derivative of f_a at the grid points can be calculated by the derivatives of S_n

$$S_n'(2(\theta_k-\theta_j))=\begin{cases} 0, & j=k, \\ \frac{1}{2}(-1)^{k+j}\cot\frac{(k-j)h}{2}, & j\neq k, \end{cases} \tag{5.5}$$

$$S_n''(2(\theta_k-\theta_j))=\begin{cases} -\frac{1}{6}-\frac{\pi^2}{3h^2}, & j=k, \\ \frac{1}{2}(-1)^{(j+k)}\csc^2\frac{(k-j)h}{2}, & j\neq k. \end{cases} \tag{5.6}$$

From the above formulas, we can construct the derivative matrices for the first through the third order derivative, respectively,

$$
\begin{aligned}
f_{a\theta,k} &= (D_n)_{kl} f_l, \quad k=-n/2,\cdots,n/2-1, \\
f_{a\theta\theta,k} &= (D_n^{(2)})_{kl} f_l, \quad k=-n/2,\cdots,n/2-1, \\
f_{a\theta\theta\theta,k} &= (D_n)_{kl}^3 f_l, \quad k=-n/2,\cdots,n/2-1,
\end{aligned}
\tag{5.7}
$$

where the derivative matrices are given by

$$
(D_n)_{ij}=2\begin{cases} 0, & i=j, \\ \dfrac{1}{2}(-1)^{i+j}\cot\dfrac{(i-j)h}{2}, & i\neq j, \end{cases}
\tag{5.8}
$$

$$
(D_n^{(2)})_{ij}=4\begin{cases} -\dfrac{1}{6}-\dfrac{\pi^2}{3h^2}, & j=i, \\ \dfrac{1}{2}(-1)^{(j+i+1)}\csc^2\dfrac{(i-j)h}{2}, & j\neq i. \end{cases}
\tag{5.9}
$$

The third order derivative is calculated by D_n^3. The second moment tensor is approximated by quadratures, for example, the composite trapezoidal rule:

$$
\mathbf{Q}=h\sum_{j=-n/2}^{n/2-1}(\mathbf{mm})_j f_j,
\tag{5.10}
$$

where the transpose of $\mathbf{m}$ evaluated at the jth grid point is given by

$$
\mathbf{m}_j^T=(\cos\theta_j,\sin\theta_j),
\tag{5.11}
$$

and the periodicity of the second moment tensor and the pdf is exploited. In the chemical potential μ_{nr}, we evaluate the second order tensor

$$
A=-N(1-\phi)\left[h\sum_{j=-n/2}^{n/2-1}(\mathbf{mm})_j f_j\right]+\frac{\beta\phi}{\alpha}\mathbf{U}.
\tag{5.12}
$$

Then, $\mu_{nr}=A:\mathbf{mm}$. The Smoluchowski equation is fully discretized at each grid point θ_j, $j=-n/2,\cdots,n/2-1$,

$$
\left[\frac{\partial}{\partial t}f_a+\mathbf{v}\cdot\nabla f_a\right]_j=\left[\frac{\partial}{\partial\theta}\frac{D_r}{kT}[f_a\frac{\partial\mu_{nr}}{\partial\theta}]-\mathbf{m}_\perp\cdot\frac{\partial}{\partial\theta}[(\mathbf{W}\cdot\mathbf{m}+a(\mathbf{D}\cdot\mathbf{m}-\mathbf{D}:\mathbf{mmm}))f_a]\right]_j,
\tag{5.13}
$$

for $j=-n/2,\cdots,n/2-1$. The equation for the structure tensor $\mathbf{U}$ is an ordinary differential equation coupled to the Smoluchowski equation. In the numerical scheme, the two systems are integrated simultaneously using a second order Runge-Kutta scheme of good A-stability. All computational results presented below are obtained for $n=64$ unless specified otherwise.

6 Numerical results

We next study the solution of the Smoluchowski equation and the polymer structure tensor equation numerically with respect to the various material parameters. We first investigate the equilibria or the steady states of the Smoluchowski equation absent of external flows ($Pe\!=\!0$).

6.1 Equilibria: effects due to nanorod semi-flexibility and nanorod-polymer surface interaction

All equilibria of the nanorod Smoluchowski equation and the corresponding polymer Smoluchowski equation are invariant under a planar rotation; this is the classical rotational degeneracy of the nematic rod phase in equilibrium which extends to the polymer-nanorod mixture. Ordered equilibria constitute a 1-parameter family; we represent each circle of ordered equilibria by fixing the peak of the nematic phase PDF at $\frac{\pi}{2}$. We remark that due to the coupling of the nanorod with the flexible polymer in the mixture, the rotational degeneracy of the nanorod and polymer Smoluchowski equation is not independent! The dual orientation of the nanorod ensemble and the polymer matrix are measured by the scalar order parameter s of the nanorod and the scalar order parameter s_u of the polymer matrix, respectively,

$$s=\sqrt{2(\mathbf{Q}-\mathbf{I}/2):(\mathbf{Q}-\mathbf{I}/2)}, \quad s_u=\sqrt{2(\mathbf{U}/tr(\mathbf{U})-\mathbf{I}/2):(\mathbf{U}/tr(\mathbf{U})-\mathbf{I}/2)}. \qquad (6.1)$$

Here, $tr(\mathbf{U})$ denotes the trace of tensor $\mathbf{U}$. Both s and s_u measure the deviation of the orientation/structure tensor from the isotropic state. Their values are confined between 0 and 1.

In this numerical study, we limit our attention to a small set of model parameters and their influence on the solution of the Smoluchowski equation with the primary focus on the modeling advances developed in this paper, which are captured by the rod semi-flexibility parameter r_f and the rod-polymer surface interaction parameter β. The following dimensionless parameter values are fixed in all calculations:

$$\Lambda_1=0.5, \quad \phi=0.9, \quad N=60, \quad E_p=50, \quad De=1, \quad \zeta=0.5, \quad \zeta_2=0.5, \quad Re=1, \quad \alpha=100.$$

We use a perturbed isotropic state as the initial condition in the transient calculations. All calculations are terminated after they demonstrate convergence to steady states. We set the convergent criterion as the difference of the pdf at two consecutive time steps to be less than 10^{-7} in the L_2 norm. We note that the time to reach steady state is not sensitive to the value of r_f, however it is sensitive to the value of β, which parameterizes the interaction between the nanorod and the host polymer matrix.

The typical steady state solution is either a pdf of uniform distribution or one of a single peak in the domain of the orientation angle θ, indicating an isotropic phase or a

nematic phase, respectively. The isotropic phase is obtained at lower values of the effective strength of the excluded volume potential $N(1-\phi)$ while the nematic one can be observed at higher values of $N(1-\phi)$. Like in any anisotropic fluids, where the concentration of the anisotropic inclusion can induce a phase transition, this model predicts a second order phase transition from the isotropic phase to the nematic phase at a critical effective strength of the excluded volume potential $N(1-\phi)$ [17]. For instance, the critical value is $N(1-\phi)=3.96$ at $r_f=0.15$.

A representative phase diagram describing the phase transition is depicted in Fig. 1 at four selected values of r_f.
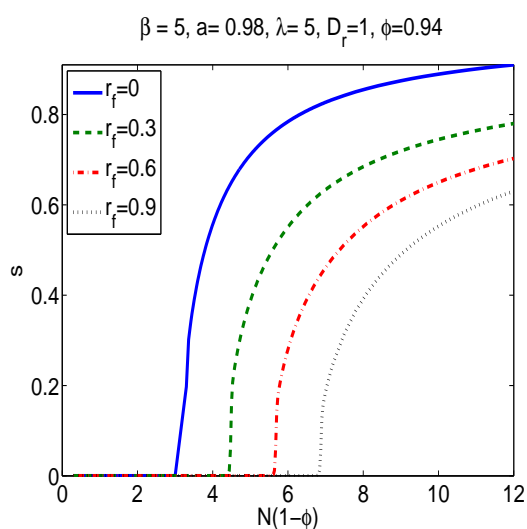

Figure 1: The bifurcation diagram of the nanorod orientational order parameter s as a function of the effective concentration $N(1-\phi)$ at selected values of the rod semi-flexibility parameter r_f. The effect of increasing r_f is shown to delay the formation of the nematic phase in the nanocomposite to higher concentration.

6.1.1   Effect of semi-flexibility of the nanorod

At fixed surface interaction parameter β, the peak of the pdf solution is lowered as r_f increases, indicating the enhanced semi-flexibility of the nanorod reduces the local degree of orientation or the mesoscale nematic order in the composite at a given nanorod concentration. The effective phase transition concentration shifts to large values as r_f increases (shown in Fig. 1). This behavior is universal for both positive and negative values of β. We note that a positive value of β promotes the perpendicular configuration of the polymer relative to the rod; while a negative one favors the parallel alignment. Fig. 2 depicts some representative steady states at selected r_f for $\beta<0$. As the nanorod semiflexibility increases, the nematic order in the nanorod ensemble reduces and the alignment in the host polymer matrix relaxes as well. Similar behavior had been reported for semiflexible liquid crystal polymers in the past [15].
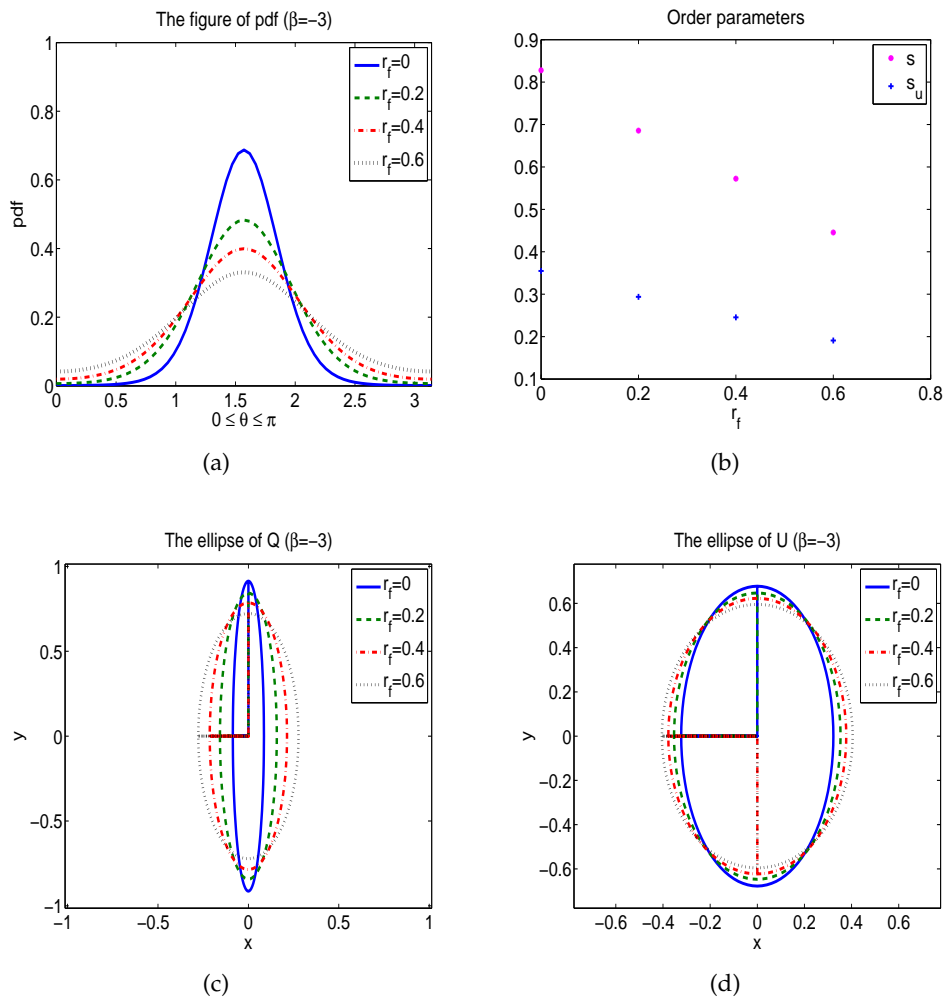
Figure 2: (a). The equilibrium pdf at four selected values of r_f. The other parameters used are $\beta=-3, N=60, \phi=0.9$. (b). Order parameter s and s_u. The orientation order in the polymer matrix is considerably lower than that in the nanorod phase in all cases. (c). The orientation tensor depicted as an ellipse, where the semiaxes are in the eigenvector directions and the length of the semiaxes represents the size of the corresponding eigenvalues. (d). The structure tensor **U** depicted as ellipses. The increase in semiflexibility of the nanorod reduces the local degree of orientation of the nanorod phase as well as that of the host polymer matrix. But, it has a weaker impact on the host polymer matrix. The major director of the orientation tensor **Q** and that of the structure tensor are parallel to each other in this case.

6.1.2 Effect of surface interaction parameter β

At a fixed value of the semi-flexibility parameter r_f, the effect of the surface interaction parameter β on the nanorod orientational order is nominal, yet the polymer matrix is modified significantly! We refer to Fig. 3. It shows that the mesostructure of the polymer matrix is quite sensitive to the interaction parameter. When $\beta > 0$, increasing β enhances
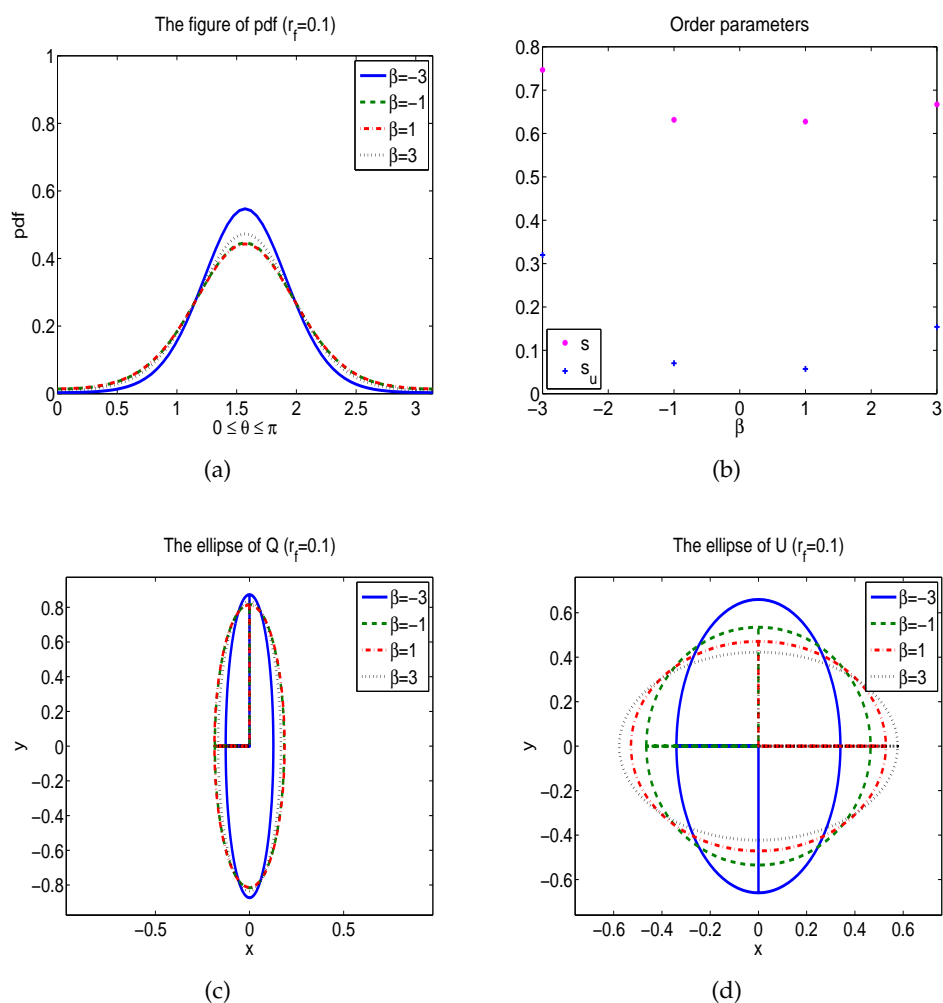
Figure 3: (a). The equilibrium pdf solution at four selected values of β. The other parameters are $r_f = 0.1, N = 60, \phi = 0.9$. (b). Order parameter s and s_u. Notice that the orientation order in the polymer matrix is considerably lower than that in the nanorod phase. (c). The orientation tensor depicted as an ellipse. (d). The structure tensor **U** depicted as an ellipse. The larger positive value of β promotes the perpendicular orientation between the nanorod and the polymer; whereas the smaller negative value of β facilitates the parallel alignment between the two.

the polymer alignment transverse to the orientation of the nanorod ensemble; whereas decreasing β when $\beta < 0$ boosts the parallel alignment of the polymer with the nanorod. The polymer matrix structure is more sensitive to the variation of β when it is negative than when it is positive.

Fig. 4 depicts the equilibrium phase diagram as a function of the effective concentration $N(1-\phi)$ at a few selected values of β in all cases. A second order phase transition is observed at critical values of the effective concentration $N(1-\phi)$ at fixed β. When
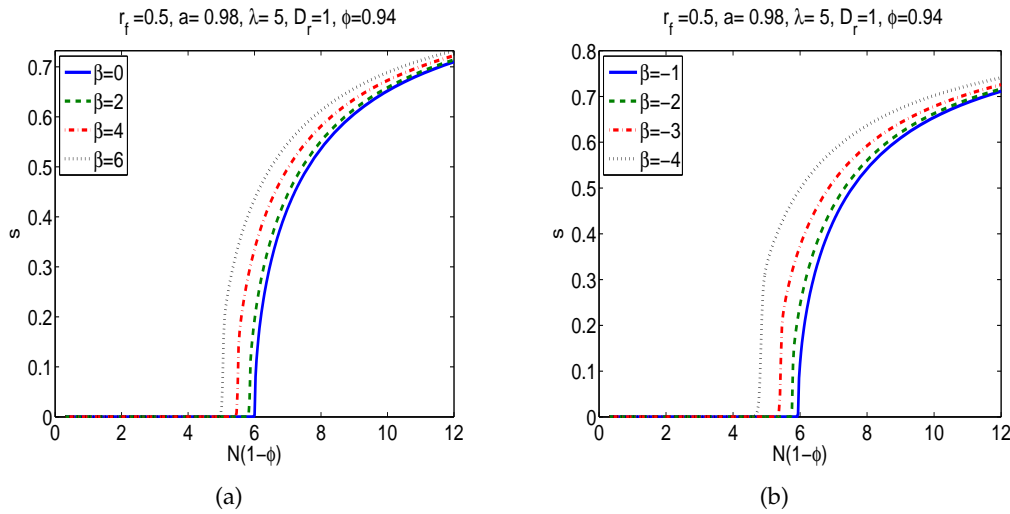
Figure 4: The bifurcation diagram of the nanorod order parameter s as a function of $N(1-\phi)$. (a). $\beta>0, r_f=0.5$, (b). $\beta<0, r_f=0.5$. The stronger surface contact interaction lowers effective phase transition concentration.

$N(1-\phi)$ is less than the critical value, the only existing phase is the isotropic one. Whenever $N(1-\phi)$ exceeds the critical value, the only stable phase is the nematic one. This phase transition phenomenon is the reminiscence of the liquid crystal polymer phase behavior [3]. Increasing $|\beta|$, i.e., enhancing the nanorod polymer interaction, promotes the nematic phase formation. It clearly establish that the phase transition value of $N(1-\phi)$ varies opposite to the variation of $|\beta|$.

We next look into the phase behavior when a linear flow of elongation or shear is imposed, respectively. As we noted in [11,13] that both types of flows are in fact potential in 2-D so that the numerical code developed here can be applied to both cases with minimal modification.

6.2 Planar elongation

When planar elongation is imposed, the rotational symmetry in the Smoluchowski equation is broken. The pdf solution no longer possesses the translational invariance with respect to the angle variable θ. In polar coordinates, the potential of the planar elongational flow is given by

$$V_{el} = \frac{aPekT}{2}\cos2\theta. \tag{6.2}$$

Elongation is a strong flow, in which all the sustainable solutions are stable steady states, so that the principal axes of both the orientation tensor and the structure tensor align with the axes of symmetry of the flow. The flow certainly aligns the polymer matrix to the flow
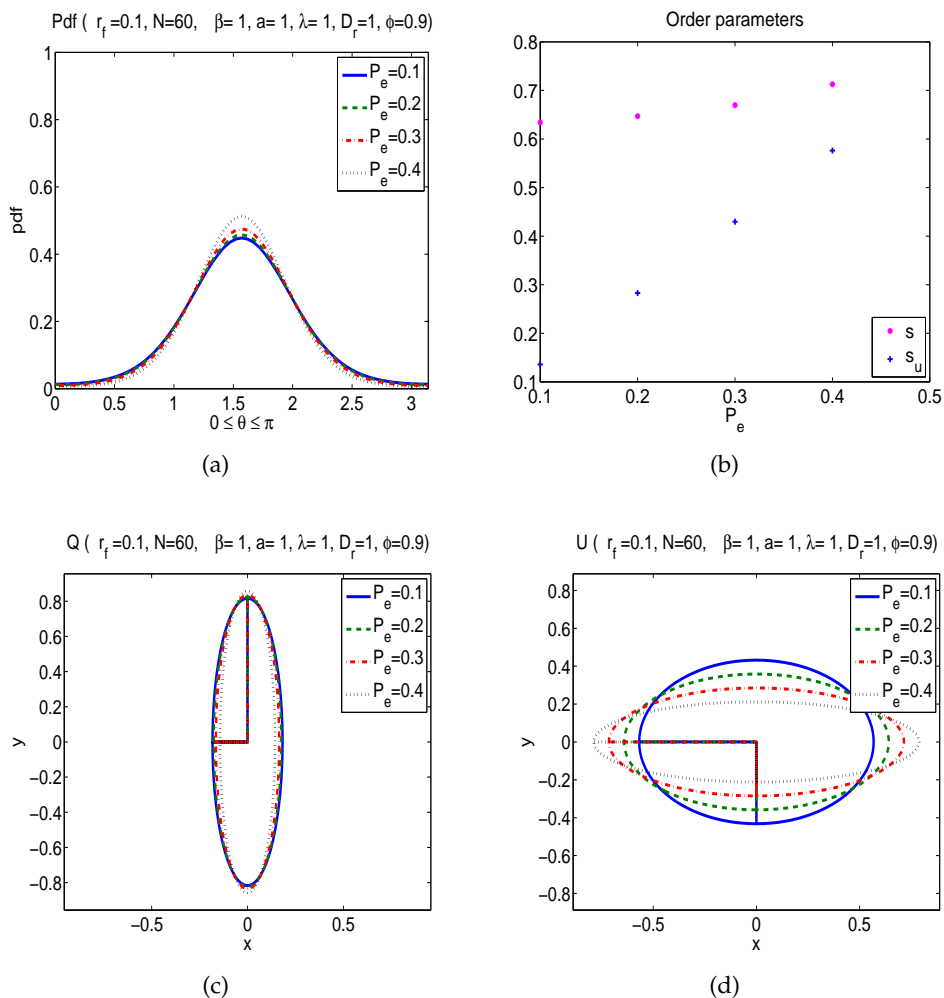
Figure 5: Steady states in elongation at various Pe, where $r_f = 0.1, \beta = 1$. (a). The steady state pdf. (b). The order parameters s and s_u. (c). The corresponding orientation tensor **Q** depicted as an ellipse. (b). The structure tensor **U** depicted as an ellipse. The enhanced elongation improves nanorod alignment nominally whereas polymer alignment significantly.

direction (i.e. the stretching direction or the x-axis in this paper). However, the nanorod alignment is slaved by the detail of the nanorod-polymer interaction at regime of small nanorod volume fraction of industrial interest. When $\beta > 0$, the interaction favors an orthogonal alignment between the nanorod phase and the flow-aligning polymer matrix; otherwise, the nanorod phase aligns with the polymer matrix in the flow direction.

Fig. 5 depicts a set of steady states at various values of the Peclet number, in which the polymer phase aligns weakly in the flow direction while the nanorod phase aligns in the flow gradient direction at $\beta = 1$. The mesoscopic order in both phases increase
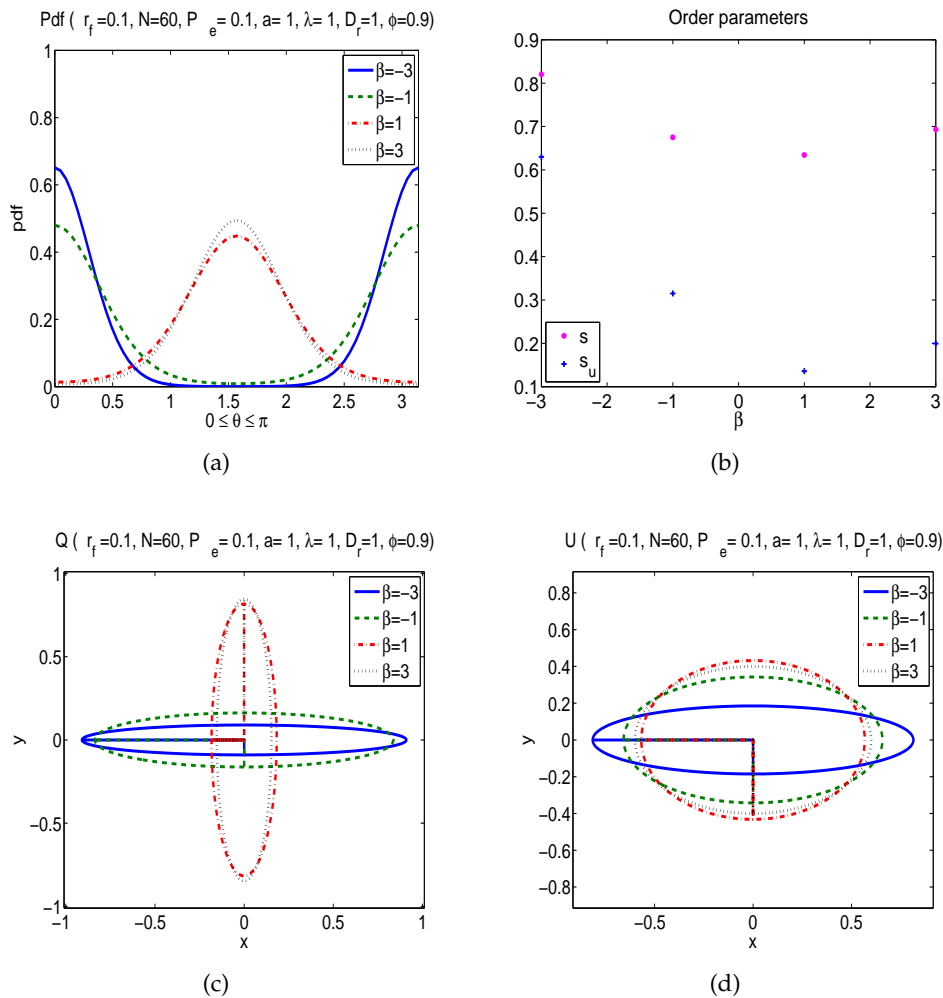
Figure 6: Steady states at various β, where $P_e = 0.1, r_f = 0.1$. (a). The steady state pdf. (b). Order parameter s and s_u. (c). The orientation tensor **Q**. (d). The structure tensor **U**. The change of β from positive to negative switches nanorod mesoscopic orientation from transverse to parallel with respect to the polymer matrix orientation, i.e., flow direction.

with the Peclet number, as expected. The enhancement in the mesoscopic order is most pronounced in the polymer matrix though. The impact of β on the nanorod ensemble and the polymer matrix is stronger in the case of $\beta < 0$ than in the case of $\beta > 0$ evidenced in Fig. 6. In the case of $\beta < 0$, the nanorod along with the polymer matrix align with the flow and the degree of orientation in the polymer matrix is enhanced significantly due exclusively to the nanorod-polymer interaction.

Analogous to the equilibrium situation, the enhancement of semi-flexibility reduces the local nematic order. However, it has a weak effect on the structure of polymeric matrix
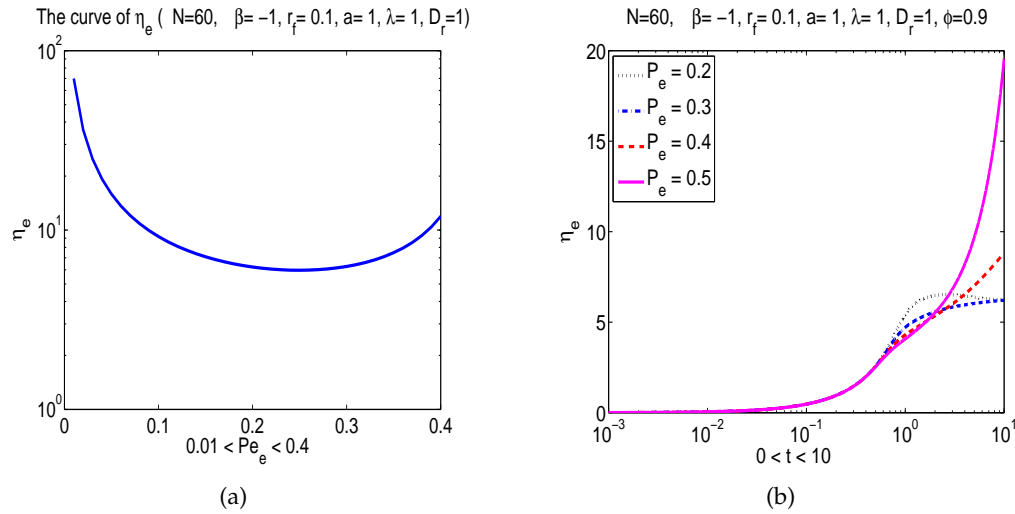
Figure 7: Steady and transient elongational viscosity. (a). The steady state elongational viscosity as a function of P_e at $\beta < 0$. Elongational thinning is seen at small Pe while elongational hardening is observed at large Pe. (b). The transient elongational viscosity as a function of time at $\beta < 0$.

in elongation in stark contrast to the significant effect of β to the nematic orientation of the nanorod and the orientational structure of the polymer matrix. This is apparently related to the low volume fraction of the nanorod considered in the paper. This scenario perhaps will change if we reverse the ratio of the volume fraction of the two components in the composite, a case which we will not explore due to the lack of scientific and industrial interest so far.

A typical steady state elongational viscosity defined by

$$\eta_e = \frac{\tau_{11} - \tau_{22}}{Pe} \tag{6.3}$$

is depicted in Fig. 7(a) as a function of the Peclet number at a set of fixed parameter values. The steady elongational viscosity decreases at small Pe, but increases at larger Pe showing a nonmonotonic trend. The transient viscosity increases with respect to time and "blows up" at some intermediate time (Fig. 7(b)).

6.3 Plane shear

Next, we study the microstructural response of the nanocomposite with respect to an imposed planar shear flow. The plane shear in 2-D is a potential flow with the potential given by

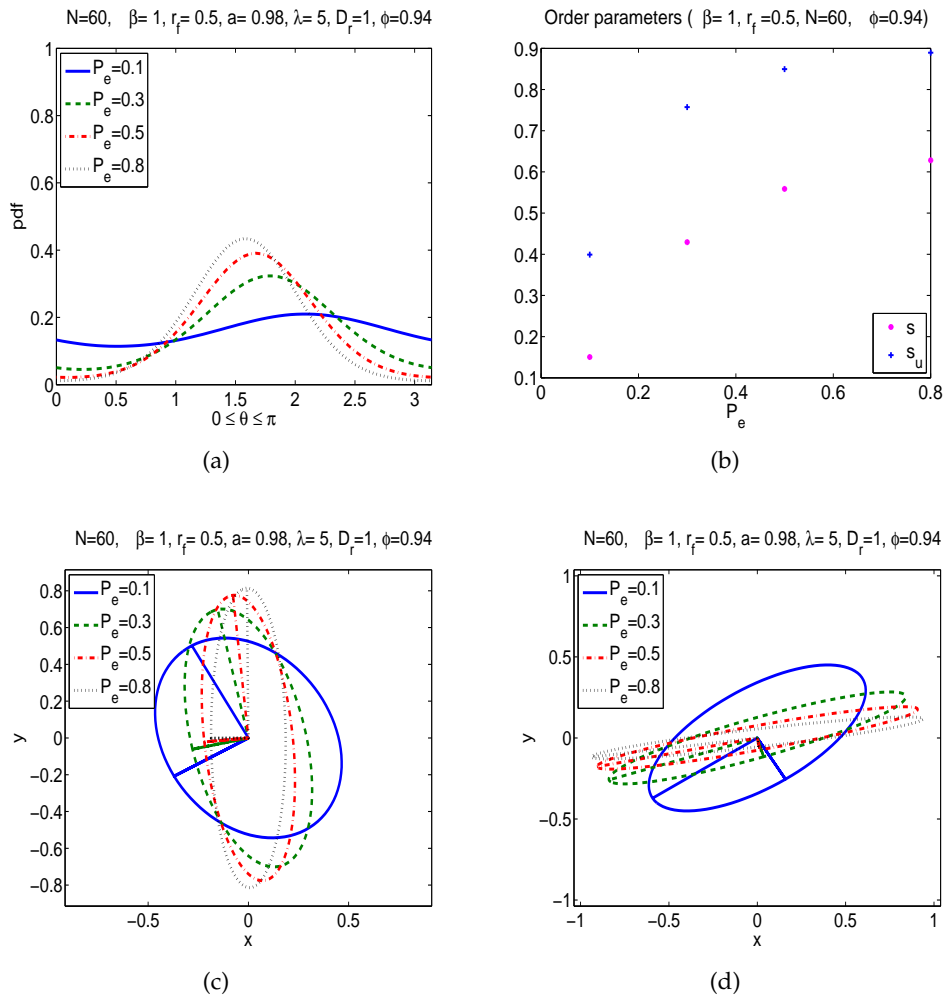$$V_{shear} = -\frac{PekT}{2}\left(\frac{a}{2}\sin 2\theta - \theta\right) \tag{6.4}$$

Figure 8: The pdf solution and the nanorod nematic orientation tensor **Q** and polymer structure tensor **U** for various values of P_e in shear. (a). PDF solution. (b). The scalar order parameters s and s_u. (c). The ellipses of **Q**. (d). The ellipses of **U**.

in polar coordinates. The nanorod kinetic equation admits either steady or time-periodic solutions in various regimes of the parameter space. It's been shown numerically that a smaller geometrical parameter a (or a fatter nanorod geometry) tends to promote the formation of time-periodic solution in liquid crystal polymer systems [14]. We will show that this feature is retained in the current PNC model. At small and large values of the effective concentration $N(1-\phi)$, steady states prevail for all Pe. Whereas, time-periodic solutions exist at intermediate range of $N(1-\phi)$ and Pe. The time-periodic solution is a feature reminiscent of the intermediate to concentrated nanorod fluids due to the excluded volume interaction [14].
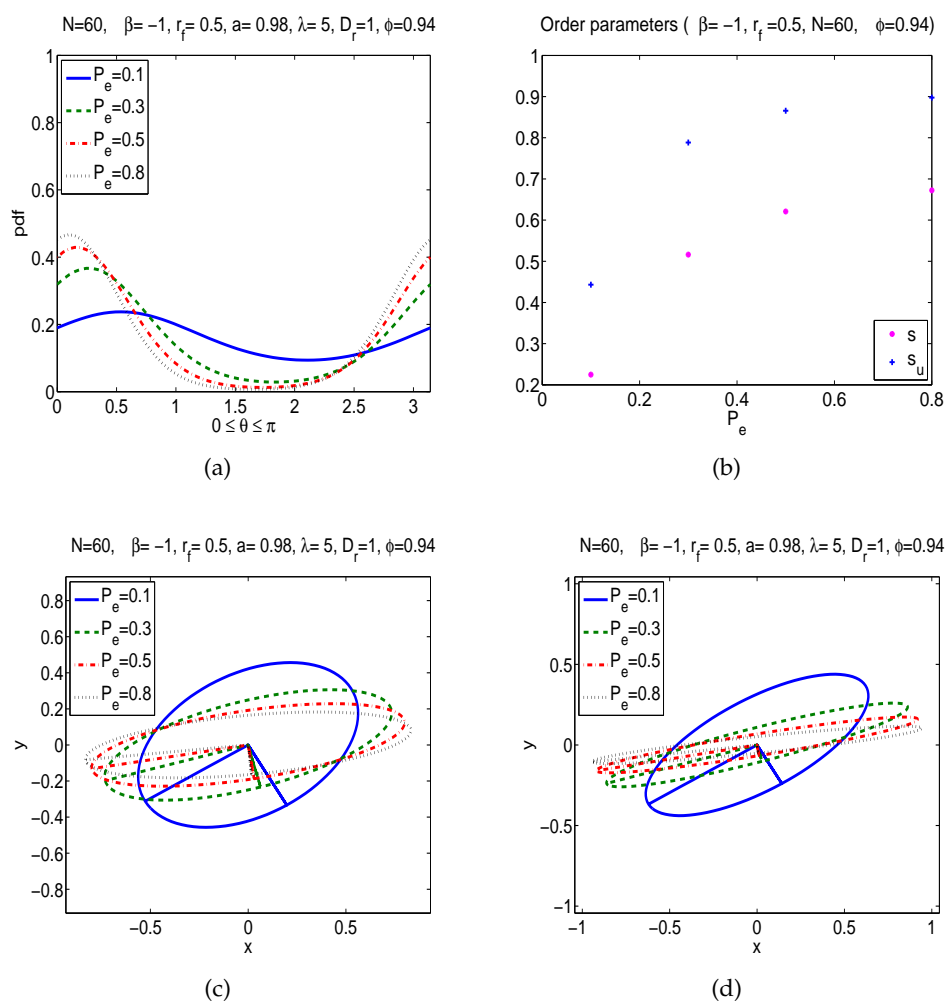
Figure 9: The pdf solution and **Q** and **U** for various values of P_e in shear. (a). PDF solution. (b). The scalar order parameters s and s_u. (c). The ellipses of **Q**. (d). The ellipses of **U**.

6.3.1   Steady state behavior

First, we study the parameter dependence of the steady states. Like in the case of elongational flows, the mesoscopic orientation of the nanorods is slaved by the polymer matrix meso-structure primarily due to the overwhelming volume advantage of it. As we increase the Peclet number, the local nematic order in both nanorod and polymer distribution improves. It is more significant in the polymer matrix than in the nanorods though. Because the polymer nanorod interaction favors a mutually orthogonal orientation between the nanorod and the polymer matrix when $\beta > 0$, the Leslie angle that the major director of the nanorod ensemble makes with the flow direction tends to be an abtuse
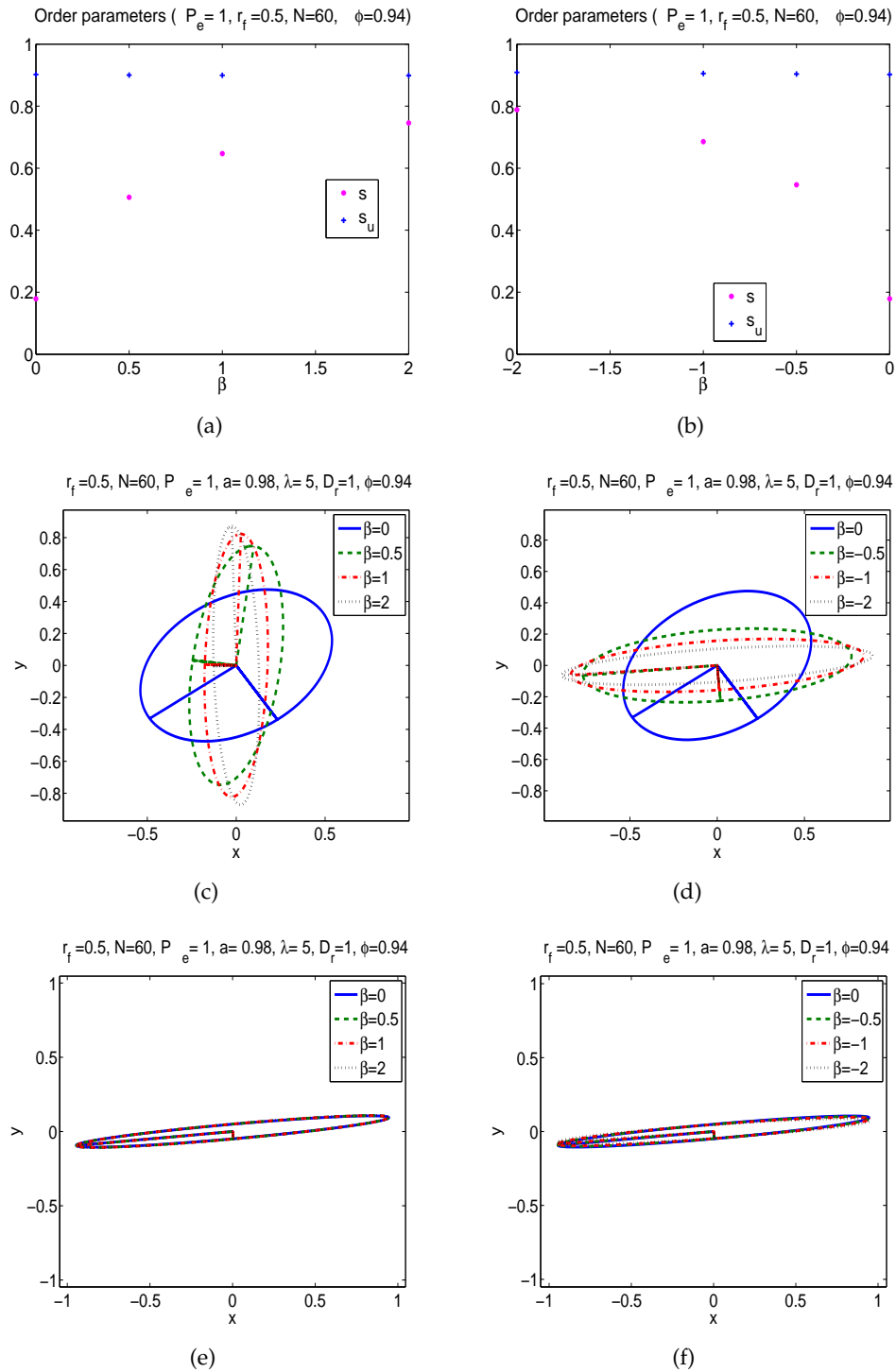
Figure 10: The pdf solution and **Q** and **U** for various values of β in shear. (a). & (b). The scalar order parameters s and s_u. (c). & (d). The ellipses of **Q**. (e). & (f). The ellipses of **U**.

one while the polymer principal axis makes a positive acute angle with the flow direction. As the Peclet number increases, the polymer principal axis tends to rotate clockwise toward the flow direction while that of the nanorod tends to rotate clockwise as well (see Fig. 8), first toward the velocity-gradient at small Peclet numbers and then toward the flow direction at large Peclet numbers. In any case, the two principal axes are neither completely orthogonal nor completely parallel in shear. The direction cosine between the two major director takes on a numerical value between zero and 1. When $\beta < 0$, it favors a nearly parallel alignment between the nanorods and the polymers. Enhanced shear strength forces the degree of order in both the nanorod ensemble and the polymer matrix to increase and their principal axes oriented towards the flow direction (see Fig. 9). The direction cosine between the two major directors is slightly less than one. The effect of semiflexibility parameter r_f on the steady state in shear is analogous to what we have alluded to in equilibrium and elongation: the major director orientation does not change much except that the local nematic order of the nanorods reduces as the semi-flexibility enhances.

When we vary the surface interaction parameter β, however, the mesoscale degree of orientation and the polymer matrix both get improved. As $|\beta|$ increases and Pe is fixed, the major director of the nanorod rotates toward the flow direction for $\beta < 0$ or the velocity-gradient direction for $\beta > 0$ while the nematic order increases sharply. Fig. 10 depicts the steady state variation with respect to β. An increase in $N(1-\phi)$ improves alignment noticeably in the degree of orientation in the nanorods yet with a nominal impact on the polymer matrix. The weakly order reducing effect of r_f and the strong order enhancement due to the increase of surface interaction (i.e., $|\beta|$) retains.

6.3.2 Rheological functions

The steady state shear viscosity, defined by $\eta_s = \tau_{xy}/Pe$, shows shear thinning behavior consistently. Fig. 11 depicts both the shear stress τ_{xy} and the normal stress difference $\tau_{xx} - \tau_{yy}$ in steady and transient flows, respectively. It shows that the normal stress difference also decreases with Pe. Transient shear viscosity and normal stress difference demonstrates a sequence of actions: initial climbing, overshooting and then reaching a plateau (See Fig. 11). Some transient oscillation is more noticeable at large Peclet numbers than others but otherwise nonexistent at small Peclet numbers. The normal stress difference oscillation is in sync with that of the shear stress component.

The shear viscosity prediction qualitatively captures the behavior observed in experiment [28, 29]. Fig. 12 shows a good agreement with the experimental data at the smaller end of the Peclet number [20, 28]. However, the prediction using the same results at large Peclet numbers yields some oscillations which seem to be larger than what was reported in experiments [28, 29]. When N, r_f and $\beta > 0$ vary respectively, the qualitative impact on the viscosity is minimal. However, variation in $\beta < 0$ does show noticeable impact on the enhancement of the overshoot in the viscosity.

Another rheological function for the nanocomposite is the small amplitude viscoelasticity, which is characterized by the elastic or storage modulus G' and the loss modulus
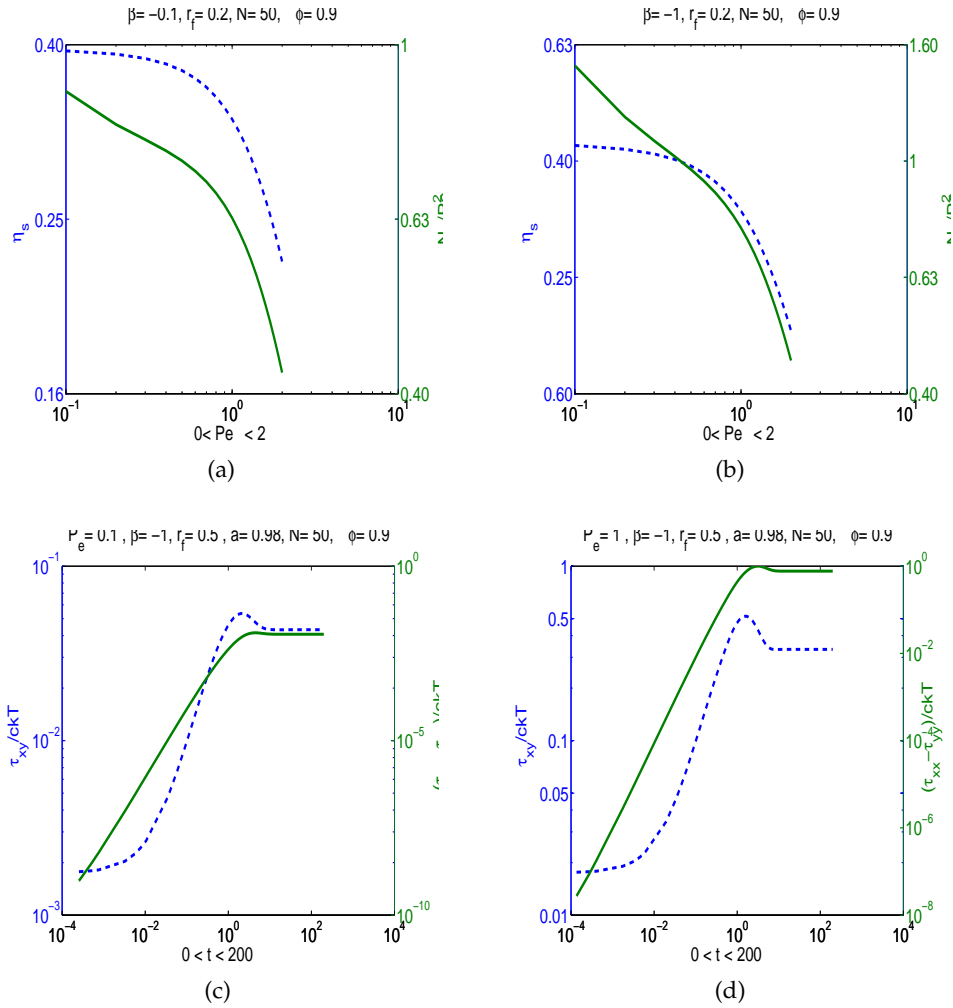
Figure 11: Shear viscosity of steady states as a function of Pe and transient shear viscosity as function of time at two selected β. The label of the dashed curve is on the left while that of the solid one is on the right. (a). Steady state viscosity and normal stress difference for $\beta > 0$. (b). Steady state viscosity and normal stress difference for $\beta > 0$. (c). Steady state viscosity and normal stress difference for $\beta < 0$. (d). Steady state viscosity and normal stress difference for $\beta < 0$.

G'', respectively. We impose the shear velocity field as follows

$$\mathbf{v} = (y\epsilon\cos\omega t, 0) \tag{6.5}$$

where $|\epsilon| \ll 1$. We linearize the stress constitutive equation about the steady state. The linearized shear stress equation can then be written into

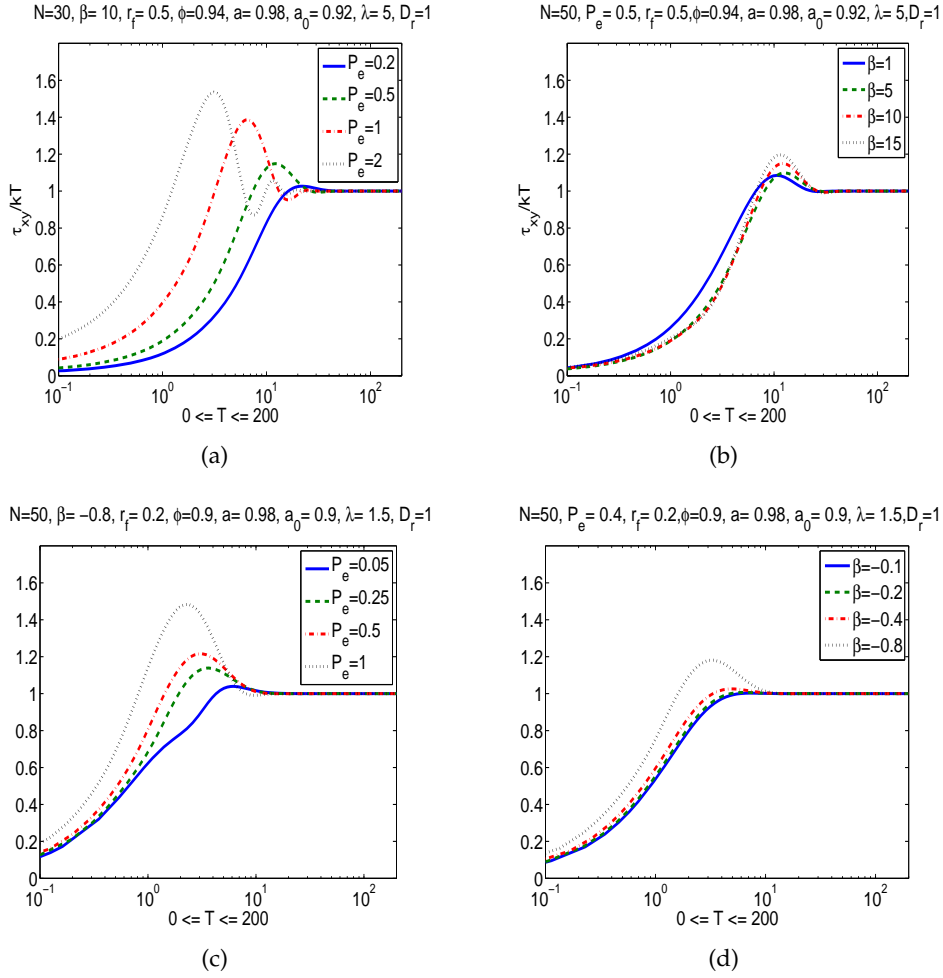$$\tau_{xy} = \frac{\epsilon}{\omega}\left(G'\sin\omega t + G''\cos\omega t\right), \tag{6.6}$$

Figure 12: Transient shear viscosity for various values of P_e normalized by its terminal value at steady states. (a) & (c) and various values of β (b) & (d).

in which G' is the storage modulus and G'' is the loss modulus. In this paper, instead of linearizing the stress equation and the Smoluchowski equation, we calculate the non-linear solution and the stress in short time and then project the stress onto the Fourier subspace corresponding to the frequency ω. Namely, this is done by expanding the shear stress response into the Fourier series of the form

$$\tau_{xy} = \sum_n \left(a_n \cos n\omega t + b_n \sin n\omega t \right), \tag{6.7}$$

where

$$a_n = \frac{\omega}{\pi} \int_{T_0}^{T_0 + \frac{2\pi}{\omega}} \tau_{xy} \cos n\omega t \, dt, \quad b_n = \frac{\omega}{\pi} \int_{T_0}^{T_0 + \frac{2\pi}{\omega}} \tau_{xy} \sin n\omega t \, dt, \tag{6.8}$$
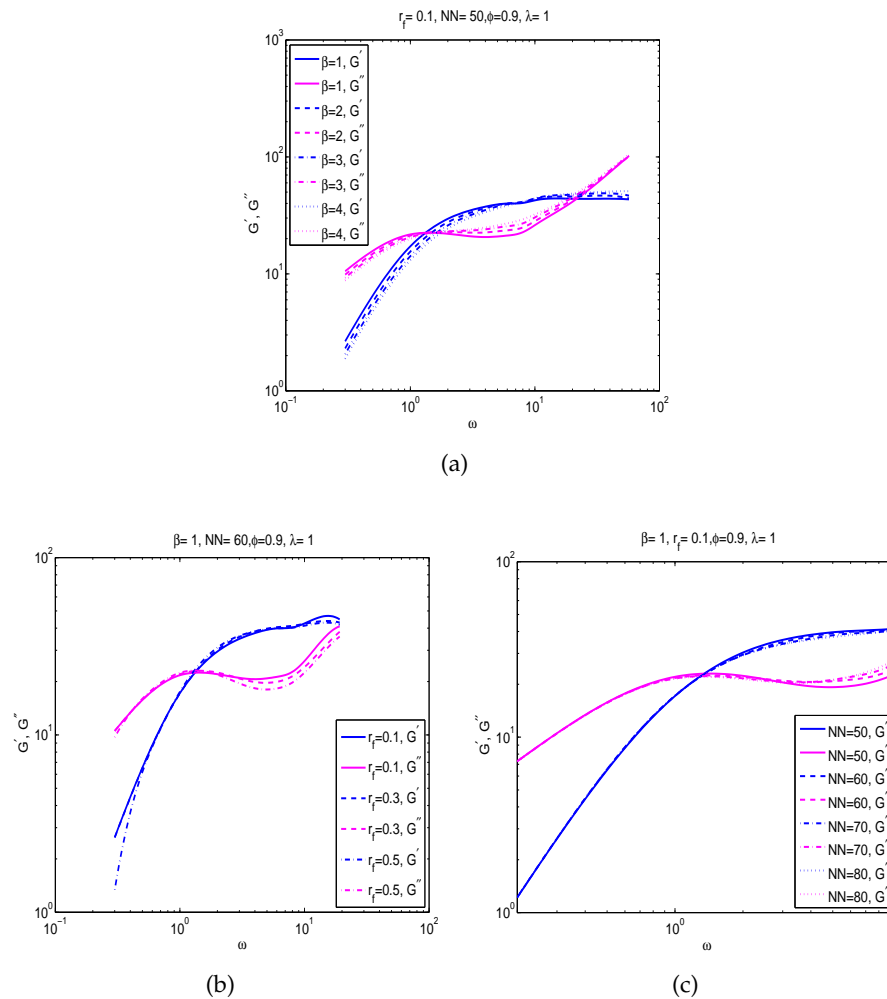
(a)

(b)   (c)

Figure 13: Storage (G') and loss (G'') modulus at various values of β, r_f, N. (a). G' and G'' at four selected values of $\beta > 0$. The slope of G' and G'' lies in $[1.7692, 1.822]$ and $[0.7874, 0.8334]$, respectively, at $\omega = 0.5$. (b). G' and G'' at three selected values of r_f. The slope of G' and G'' fluctuates slightly around 1.769 and 0.7884, respectively, at $\omega = 0.5$. (c). G' and G'' at four selected values of N. The slope of G' and G'' varies in $[1.8626, 1.8741]$ and $[0.8721, 0.8761]$, respectively, at $\omega = 0.4$.

$T_0 > 0$ is the initial transient time after which the solution exhibit periodic behavior. Then, $\epsilon G' = \omega b_1, \epsilon G'' = \omega a_1$ are recovered.

In all cases we investigated, G' and G'' demonstrate noticeable crossover behavior as the frequency increases. At low frequency, G' is smaller than G''. As the frequency increases, the difference between the two shrinks to zero and then G' takes over G'' as the larger one. This lasts for a few decades of the frequency and then the role of G' and G'' switch back. The material parameters dictate the slope of the two curves at small frequency regime, the crossover frequency, and the eventual slopes of the two curves.
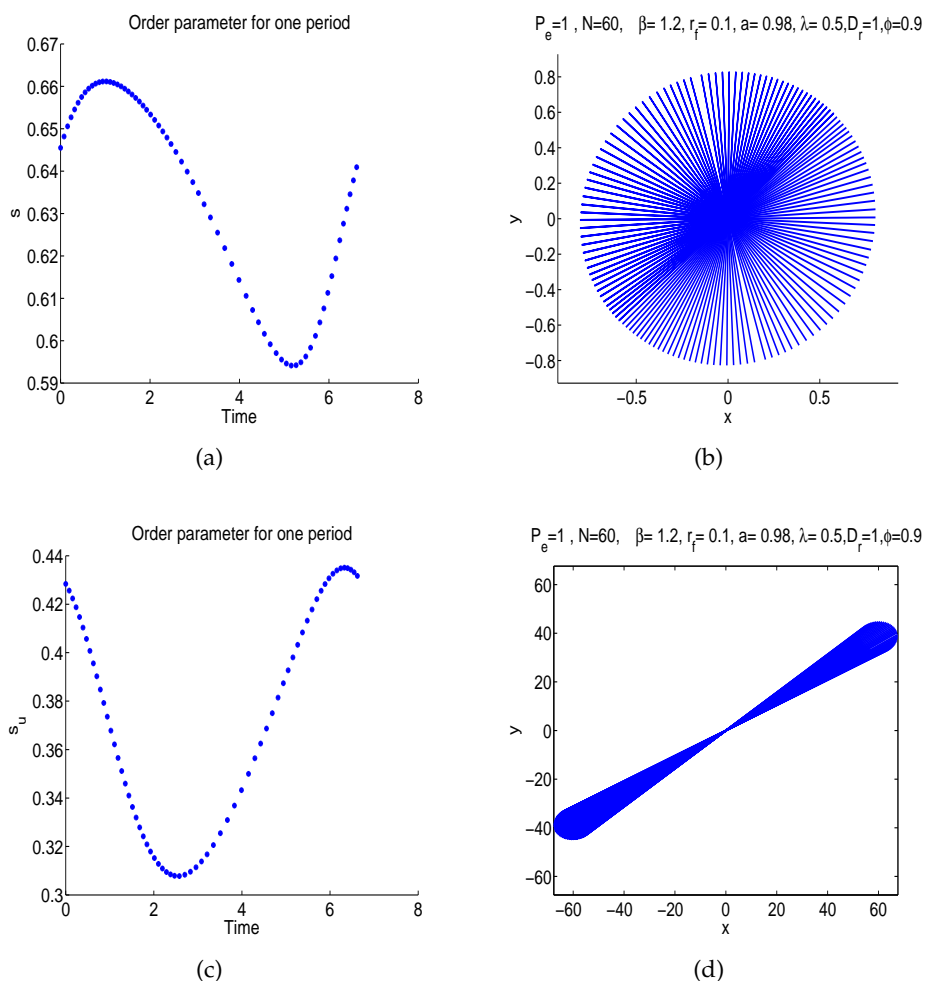
(a)

(b)

(c)

(d)

Figure 14: A tumbling solution. (a). Order parameter s over one period. (b). The tumbling major director of **Q** over one period. (c). Order parameter s_u over one period. (d). The wagging major director of **U** over one period.

These phenomena have been documented in some experiments [28, 29]. The model captures them qualitatively.

6.3.3 Time-periodic states

Time-periodic solutions exist in this system at some regimes of Pe and $N(1-\phi)$. For the time-periodic solutions, we observe either tumbling (rotating a full π circle, Fig. 14) or wagging (oscillating about a certain direction with the sway of angles less than π, Fig. 15) behavior in the nanorod ensemble. In the meantime, the polymer matrix synchronically exhibits wagging behavior. In both tumbling and wagging states, the order parameters fluctuate as well. In the tumbling case, the nematic order of the nanorod fluctuates be-
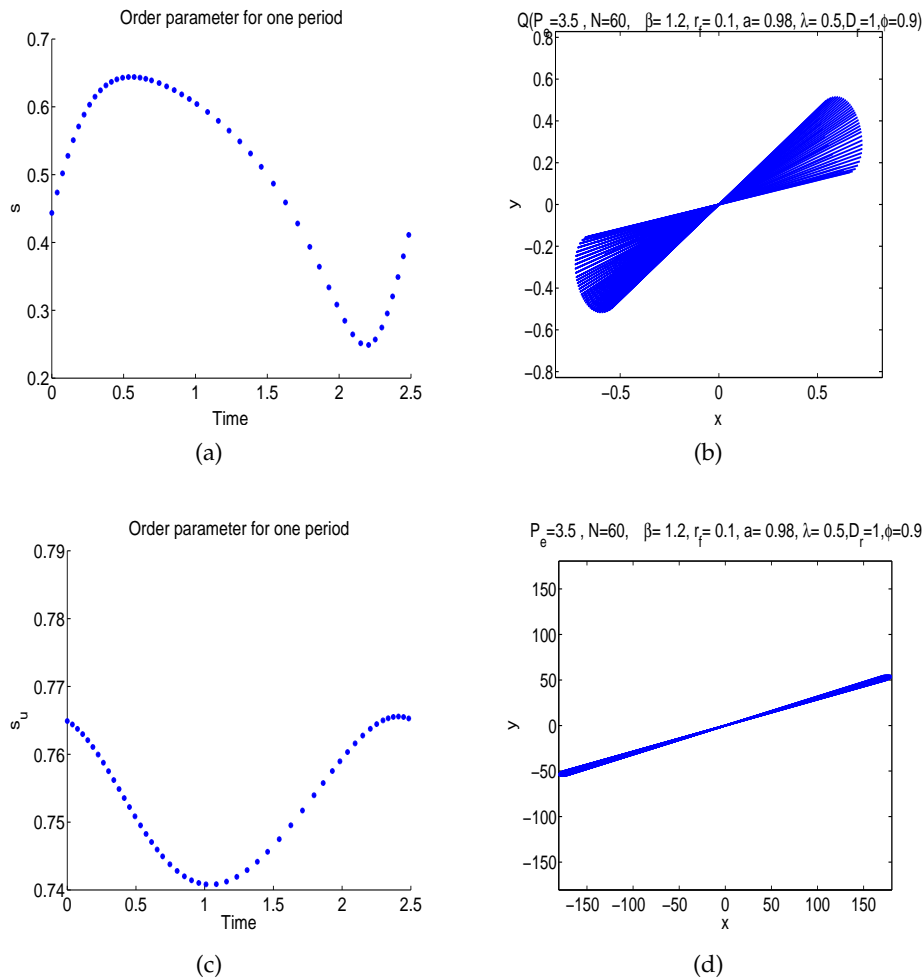
Figure 15: A wagging solution. (a). Order Parameter s over one period. (b). The waggling major director of **Q** over one period. (c). Order parameter s_u over one period. (d). The wagging major director of **U** over one period.

tween 0.59 and 0.66 while that of the polymer matrix bounces between 0.31 and 0.44 as depicted in Fig. 14. In the case of wagging, on the other hand, the nematic order oscillates between 0.24 and 0.64 while that of the polymer matrix bounces between 0.74 and 0.765 shown in Fig. 15. The local order of both the nanorod and the polymer matrix couple strongly to the director motion. The nematic order in both constituent ensembles oscillates the most when the directors wags in a large angle. The magnitude of fluctuation attenuates as the wagging angle decreases. In general, a decrease in polymer relaxation time Λ_1, an increase in the semiflexibility r_f, and a decrease in the surface interaction parameter β tend to promote steady states; large Peclet numbers also arrest time-periodic solutions to steady states. For periodic solutions, an increase in Pe and β tends to reduce
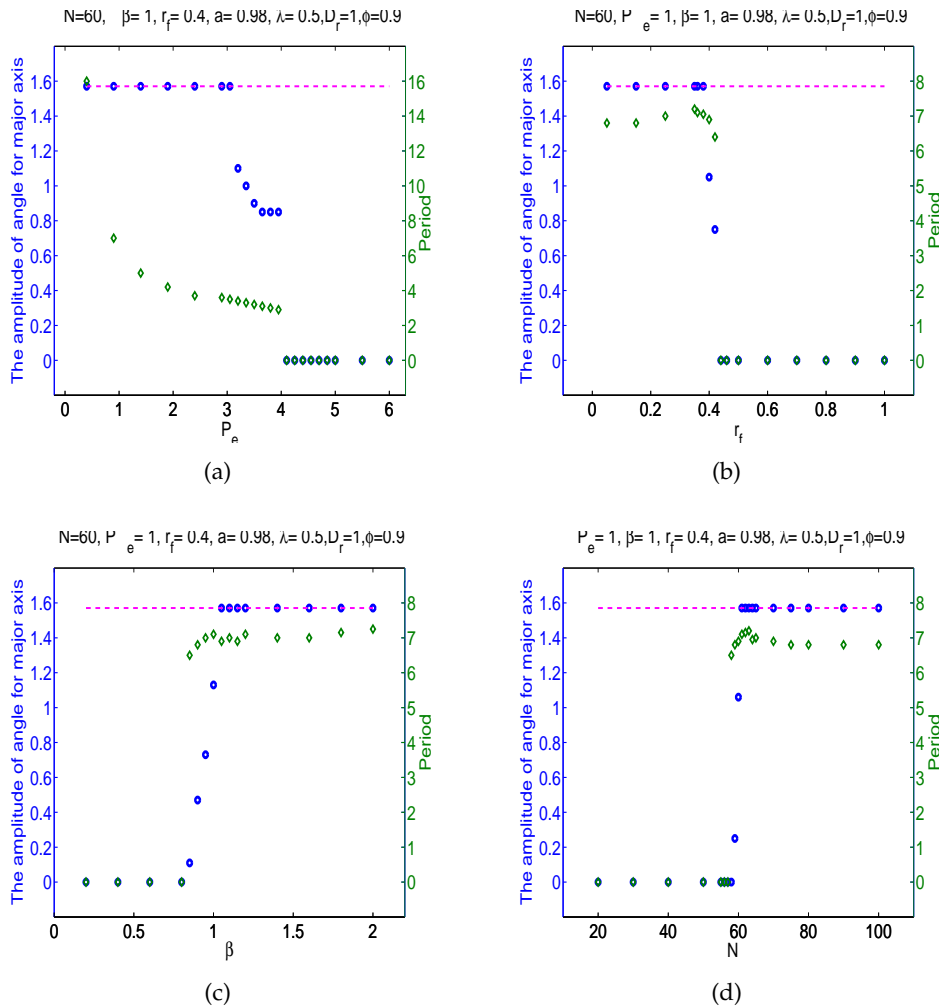
Figure 16: The half of the rotated angle of the major director and the period in the solution. The dashed line is $\pi/2$, the circles depict the half of the rotated angle of the major director, and the diamonds show the period of the solution. (a). The case of varying P_e. The wagging behavior is shown between $3.2 \leq P_e \leq 4.1$. For $P_e < 3.2$, it is tumbling and steady state for $P_e > 4.25$. (b). The case of varying r_f. It is wagging at $0.4 \leq r_f \leq 0.42$, tumbling at $r_f < 0.4$, and steady state at $r_f > 4.25$. The period peaks near the tumbling-wagging transition. (c). The case of varying β. It is wagging when $0.85 \leq \beta 1.05$, tumbling when $\beta \geq 1.05$, and steady state when $\beta < 0.85$. (d). The case of varying N. It is wagging when $59 \leq N \leq 60$, tumbling when $N \geq 61$, and steady state when $N < 59$. The period peaks near the tumbling-wagging transition.

the size of the period. In particular, a negative value of β has a strong tendency to arrest periodic solutions: at smaller negative values of β, no periodic solutions can be sustained.

Fig. 16 depicts the half of the angle rotated in the time-periodic motion and the time period in various parameter regimes. The angle rotated is a monotonic function of the parameters while the period may not. For instance, the period does not vary monotonically with respect to r_f and N. It peaks in the interval where tumbling shifts to wagging.

7   Conclusion

A hydrodynamic kinetic theory for monodomain, incompressible polymer-nanorod composites is developed merging the kinetic theory for semiflexible rod suspensions and flexible polymers [14, 15], in which details of the polymer conformation, the polymer-nanorod surface contact interaction, semiflexibility of the nanorod, and nanorod hydrodynamics are accounted for. This study explores the semiflexibility of the nanorod, the crucial nanorod-polymer coupling and its consequence to the mesoscopic structure and rheology in the quiescent state, plane elongation and shear, respectively. It shows strong impact of the polymer nanorod surface interaction to the mesoscopic structure of the nano-composite and to its rheology. The model qualitatively predicts the rheological features of PNCs in elongation and shear flow shedding light on further improvement of the modeling effort for PNCs.

Acknowledgments

References

[1] B. Bird, R. Armstrong, and O. Hassager, Dynamics of Polymeric Liquids, John Wiley and Sons, New York, 1987.

[2] C. Canuto, M. Y. Hussaini, A. Quarteroni, and T. A. Zhang, Spectral Methods Evolution to Complex Geometries and Applications to Fluid Dynamics, Springer-Verlag, Berlin-Heidelberg, 2007.

[3] M. Doi and S. F. Edwards, The Theory of Polymer Dynamics, Oxford University Press, UK, 1986.

[4] J. K. G. Dhont and W. J. Briels, Stresses in inhomogeneous suspensions, Journal of Chemical Physics, 117(8), 3992-3999 (2002).

[5] J. K. G. Dhont and W. J. Briels, Inhomogeneous suspensions of rigid rods in flow, Journal of Chemical Physics, 118(3), 1466-1478 (2003).

[6] J. K. G. Dhont and W. J. Briels, Viscoelasticity of suspensions of long, rigid rods, Colloids and Surfaces A: Physicochem. Eng. Aspects, 213, 131-156 (2003).

[7] J. K. G. Dhont, M. P. G. van Bruggen, and W. J. Briels, Long-time self-diffusion of rigid rod at low concentration: A variational approach, Macromolecules, 32, 3809-3816 (1999).

[8] W. E and P. Palffy-Muhoray, Phase separation in incompressible systems, Phys. Rev. E, 55(4), 3844-3846 (1997).

[9] Y. Dzenis, Materials science: structural nanocomposites, Science, 319(5862), 419-420 (2008).

[10] H. Eslami, M. Grmela, and M. Bousmina, A mesoscopic rheological model of polymer/layered silicate nanocomposites, J. Rhol., 51(6), 1189-1222 (2007).

[11] M. G. Forest and Q. Wang, Monodomain response of finite-aspect-ratio macromolecules in shear and related linear flows, Rheological Acta, 42, 20-46 (2003).

[12] M. G. Forest, R. Zhou, and Q. Wang, Chaotic boundaries of nematic polymers in mixed shear and extensional flows, Physical Review Letters, 93(8), 088301-088305 (2004).

[13] M. G. Forest, Q. Wang, and R. Zhou, The flow-phase diagram of Doi-Hess theory for sheared nematic polymers II: finite shear rates, Rheological Acta, 44(1), 80-93 (2004).

[14] G. Forest and Q. Wang, Hydrodynamic theories for blends of flexible polymer and nematic polymers, Phys. Rev. E, 72, 041805 (2005).

[15] A. R. Khokhlov and A. N. Semenov, Liquid-crystalline ordering in solutions of semiflexible macromolecules with rotational-isomeric flexibility, Macromolecules, 17, 2678-2685 (1984).

[16] A. J. Liu and G. H. Fredrickson, Phase separation kinetics of rod/coil mixtures, Macromolecules, 29, 8000-8009 (1996).

[17] T. C. Lubensky and P. M. Chaikin, Principles of Condensed Matter Physics, Cambridge University Press, Cambridge, 1995.

[18] P. A. Mirau, J. L. Serres, D. Jacobs, P. H. Garrett, and R. A. Vaia, Structure and Dynamics of Surfactant Interfaces in Organically Modified Clays, J. Phys. Chem. B, 112(34), 10544-10551 (2008).

[19] C. Muratov and W. E, Theory of phase separation kinetics in polymer-liquid crystal system, Journal of Chemical Physics, 116(11), 4723-4734 (2002).

[20] M. Rajabian, C. Dubois, and M. Grmela, Suspensions of semiflexible fibers in polymeric fluids, Rheology and Thermodynamics, 44(5), 521-535 (2005).

[21] R. A. Vaia and H. D. Wagner, Framework for nanocomposites, Materials Today, 7(11), 32-37 (2004).

[22] R. A. Vaia, Polymer Nanocomposites Open a New Dimension for Plastics and Composites, Report, 2005.

[23] R. A. Vaia, Nanocomposites: remote-controlled actuators, Nature Materials, 4(6), 429-430 (2005).

[24] H. D. Wagner and R. A. Vaia, Nanocomposites: issues at the interface, Materials Today, 7(11), 38-42 (2004).

[25] Q. Wang, A hydrodynamic theory of nematic liquid crystalline polymers of different configurations, Journal of Chemical Physics, 116, 9120-9136 (2002).

[26] Q. Wang, W. E, C. Liu, and P. Zhang, Kinetic theories for flows of nonhomogeneous rodlike liquid crystalline polymers with a nonlocal intermolecular potential, Phys. Rev. E, 65(5), 051504 (2002).

[27] K. I. Winey and R. A. Vaia, Polymer nanocomposites, MRS Bulletin, 32(4), 314-322 (2007).

[28] D. Wu, C. Zhou, Z. Hong, D. Mao, and Z. Bian, Study on rheological behaviour of poly(butylene terephthalate)/montmorillonite nanocomposites, European Polymer Journal, 41, 2199-2207 (2005).

[29] J. Zhao, A. B. Morgan, and J. D. Harris, Rheological characterization of polystyreneclay nanocomposites to compare the degree of exfoliation and dispersion, Polymer, 46, 8641-8660 (2005).